

https://dspace.org/

Geochronology of the Daitari Greenstone Belt Singhbhum Craton India

Jaganmoy Jodder; Thomas Hofmann; H Xie; M Elberg; Allan Wilson

ELSEVIER SCIENCE BV
https://hdl.handle.net/10539/43081
WOS

Downloaded from a DSpace repository. https://dspace.org/

Precambrian Research 388 (2023) 106997



Contents lists available at ScienceDirect

Precambrian Research

journal homepage: www.elsevier.com/locate/precamres





Geochronology of the Daitari Greenstone Belt, Singhbhum Craton, India

Jaganmoy Jodder [a,b,c,*], Axel Hofmann [a], Hangqiang Xie [d], Marlina A. Elburg [b], Allan Wilson [e]

[a] Evolutionary Studies Institute, University of the Witwatersrand, Private Bag 3, Wits 2050, South Africa
[b] Department of Geology, University of Johannesburg, PO, Box 524, Auckland Park, 2006, Johannesburg, South Africa
[c] Abteilung Isotopengeologie, Universität Göttingen, Goldschmidtstraße 1, 37077 Göttingen, Germany
[d] Beijing SHRIMP Center, Chinese Academy of Geological Sciences, 26 Baiwanzhuang Road, Beijing 100037, China
[e] School of Geosciences, University of the Witwatersrand, Johannesburg, 2000, South Africa

ARTICLE INFO

Keywords:
Singhbhum Craton
Daitari Greenstone Belt
Palaeoarchaean
3.5 Ga old felsic magmatism
Crustal evolution

ABSTRACT

The Singhbhum Craton in India contains well-preserved Palaeoarchaean greenstone belts that rival their Australian and South African counterparts, but their stratigraphic make-up remains to be resolved. Here we provide new SHRIMP- and LA-ICP-MS-based U–Pb and Lu-Hf data on magmatic and detrital zircons from stratigraphically resolved samples of the Daitari Greenstone Belt (DGB) in the south of the Singhbhum Craton. A minimum age for the Kalisagar Formation, the lowermost mafic–ultramafic volcanic suite of the DGB, is provided by a felsic sill dated at 3505 ± 6 Ma. Felsic volcaniclastic rocks from the overlying Talpada Formation provided a weighted mean age of 3507 ± 5 Ma. Zircon $\varepsilon Hf_{(t)}$ indicate a juvenile source for 3.5 Ga felsic volcanic rocks. Erosion of the volcanic edifice of the Talpada Formation acted as a predominant source for the overlying turbidite sequence of the Sindurimundi Formation, having identical U-Pb detrital zircon ages of ~ 3505 Ma. A maximum age of deposition of 3502 ± 2 Ma is proposed for the Sindurimundi Formation. Magmatic zircon ages obtained from different intrusive felsic rocks in the Daitari belt ranges from c. 3.37 to 3.35 Ga and support the notion of widespread felsic magmatism of the Singhbhum Suite in the southern part of the craton. Xenocrystic zircon crystals dated at c. 3.55 to 3.52 Ga may correspond to an earlier phase of magmatism. 3.5 Ga marks an important period in the Earth's history, when extensive felsic magmatism facilitated continental crustal growth as recorded in the Singhbhum, Kaapvaal and Pilbara cratons.

1. Introduction

Archaean granite-greenstone terrains record early Earth processes (Kröner et al., 2013; Byerly et al., 2019; Hofmann et al., 2019) and their study sheds light on the growth of Earth's primordial continental crust (Dhuime et al., 2012; Næraa et al., 2012; Reimink et al., 2014; Kamber, 2015; Bauer et al., 2020; Mulder et al., 2021; Greber et al., 2017). A few well-preserved Palaeoarchaean greenstone belts also provide clues related to habitable environments on the young Earth (Tice and Lowe, 2006a; Hofmann and Bolhar, 2007; Wacey, 2009; Homann, 2019; Sugitani, 2019) and include those from South Africa, Australia and India (Byerly et al., 2019; Agangi et al., 2018; Van Kranendonk et al., 2019; Jodder et al., 2021).

The Singhbhum Craton of India preserves a Palaeoarchaean granite-greenstone terrain overlain by a Meso- to Neoarchaean cratonic-cover sequence (Prasada Rao et al., 1964; Murthy and Acharya, 1975; Iyenger and Murthy, 1982; Acharyya, 1993; Jena and Behera, 2000; Mohakul and Bhutia, 2015; Hofmann et al., 2022). Volcano-sedimentary greenstone successions are found in the Daitari, Gorumahisani and Nausahi belts, respectively, and they are referred collectively as the Badampahar Group (Iyengar and Murthy, 1982; Jena and Behera, 2000; Hofmann et al., 2022). They range from ca. 3.53 to 3.35 Ga in age and are surrounded and intruded by tonalite-trondhjemite-granodiorite (TTG) gneisses and granites of the Singhbhum Granitoid Complex (Nelson et al., 2014; Dey et al., 2017; Mitra et al., 2019; Pandey et al., 2019; Hofmann et al., 2022; Mitra et al., 2022; Olierook et al., 2019). The Singhbhum Granitoid Complex incorporates the early, pre-tectonic Champua Suite of TTG plutons, the intermediate Singhbhum Suite of granodioritic to granitic rocks and the late, post-tectonic Mayurbhanj Suite of alkali-feldspar granites and syenites (Hofmann et al., 2022). Badamapahar Group supracrustals subjected to amphibolite facies metamorphism are found in greenstone belt remnants in the central portion of the Singhbhum Craton near Champua and Deo River (Hofmann et al., 2022).

* Corresponding author at: Evolutionary Studies Institute, University of the Witwatersrand, Private Bag 3, Wits 2050, South Africa.
E-mail address: jaganmoyj@gmail.com (J. Jodder).

https://doi.org/10.1016/j.precamres.2023.106997
Received 3 November 2022; Received in revised form 7 February 2023; Accepted 10 February 2023
Available online 24 February 2023
0301-9268/© 2023 Elsevier B.V. All rights reserved.

Detailed field, geochronological and geochemical investigation of greenstone sequences from South Africa and Australia older than 3.2 Ga over several decades led to an improved understanding of their overall stratigraphic and tectonic evolution (Viljoen and Viljoen, 1969a,b; Anhaeusser, 2014; Byerly et al., 2019; Hickman, 1983; Van Kranendonk et al., 2019). However, the Archaean geological record of the Singhbhum Craton has until recently (Hofmann et al., 2022) lacked a consistent framework that resulted in lumping together distinct lithological assemblages of Palaeoarchaean greenstone belts and Meso- to Neoarchaean cratonic cover (e.g., Saha 1994; Mukhopadhyay and Matin, 2020; Chaudhuri, 2020; Mazumder and Chaudhuri, 2021; Bhattacharjee et al., 2021; Chowdhury et al., 2021; Mazumder et al., 2022).

Despite a recent surge in early Earth research on the Singhbhum Craton, its greenstone successions lack detailed field and geochronological data (Mukhopadhyay et al., 2008; Saha et al., 2021; Hofmann et al., 2022). In fact, much less is known about the low-grade greenstone belts when compared to the amphibolite facies greenstone belt remnants in the central and northern portions of the Singhbhum Craton (Chaudhuri et al., 2018; Dey et al., 2019; Pandey et al., 2019; Upadhyay et al., 2014, 2019; Hofmann et al., 2022). So far, the only precise ages available from the Palaeoarchaean greenstone sequences of the Singhbhum Craton have been reported from felsic volcanic rocks of the Daitari and Gorumahisani belts (Mukhopadhyay et al., 2008; Sreenivas et al., 2019; Jodder et al., 2021), but a rigorous understanding of their lithostratigraphic divisions is yet to be established. The Daitari Greenstone Belt (DGB) in the south of the Singhbhum Craton (Fig. 1) exposes nearly 7 km thick Palaeoarchaean volcano-sedimentary strata (Jodder, 2021). A recent study of the volcanic rocks of the DGB reported imprecise radiometric age estimates based on whole rock Sm–Nd isochron data, i.e., 3573 ± 63 Ma from mafic-ultramafic rocks and 3507 ± 180 Ma for the felsic volcanic rocks the DGB respectively (Adhikari et al., 2021). Our goal is to improve on the understanding of the geochronological evolution of the DGB with precise age information coupled to previously published parsimonious geochronological data. Furthermore, a comparison with well-investigated greenstone belts of South Africa and Australia is attempted here.

2. Geological background

The Daitari Greenstone Belt is situated near the southern margin of the Singhbhum craton (Fig. 1). Formerly known as the Southern Iron Ore Group or Daitari–Tomka Basin, it is intruded by granitoids and unconformably overlain by the ≤ 3.0 Ga old quartzite-conglomerate succession of the Mahagiri sedimentary sequence (Acharyya, 1993; Jena and Behera, 2000; Mukhopadhyay et al., 2008). The Sukinda layered ultramafic complex (Fig. 1) exposed in the vicinity of the DGB is in inferred tectonic contact with the Mahagiri sedimentary rocks and contains stratiform chromite deposits (Mondal et al., 2006; Hofmann et al., 2022). The minimum age for both Mahagiri sedimentary rocks and the Sukinda suite is provided by NNE-oriented mafic dykes dated elsewhere in the Singhbhum Craton at c. 2.80–2.75 Ga (Kumar et al., 2017; Srivastava et al., 2019).

In the Daitari belt a ~ 7 km thick pile of volcano-sedimentary strata was mapped (Fig. 2, Jodder, 2021) and is assigned to the Palaeoarchaean Badampahar Group (Acharyya, 1993; Jena and Behera, 2000; Hofmann et al., 2022). The DGB, covering an area of ~ 60 km^2 (Fig. 1) is largely represented by mafic/ultramafic rocks, which comprise ~ 70 % of the greenstone belt. The volcano-sedimentary rocks of the DGB have been subjected to greenschist facies metamorphism and multiple phases of folding and faulting (Prasada Rao et al., 1964; Acharya, 2002;

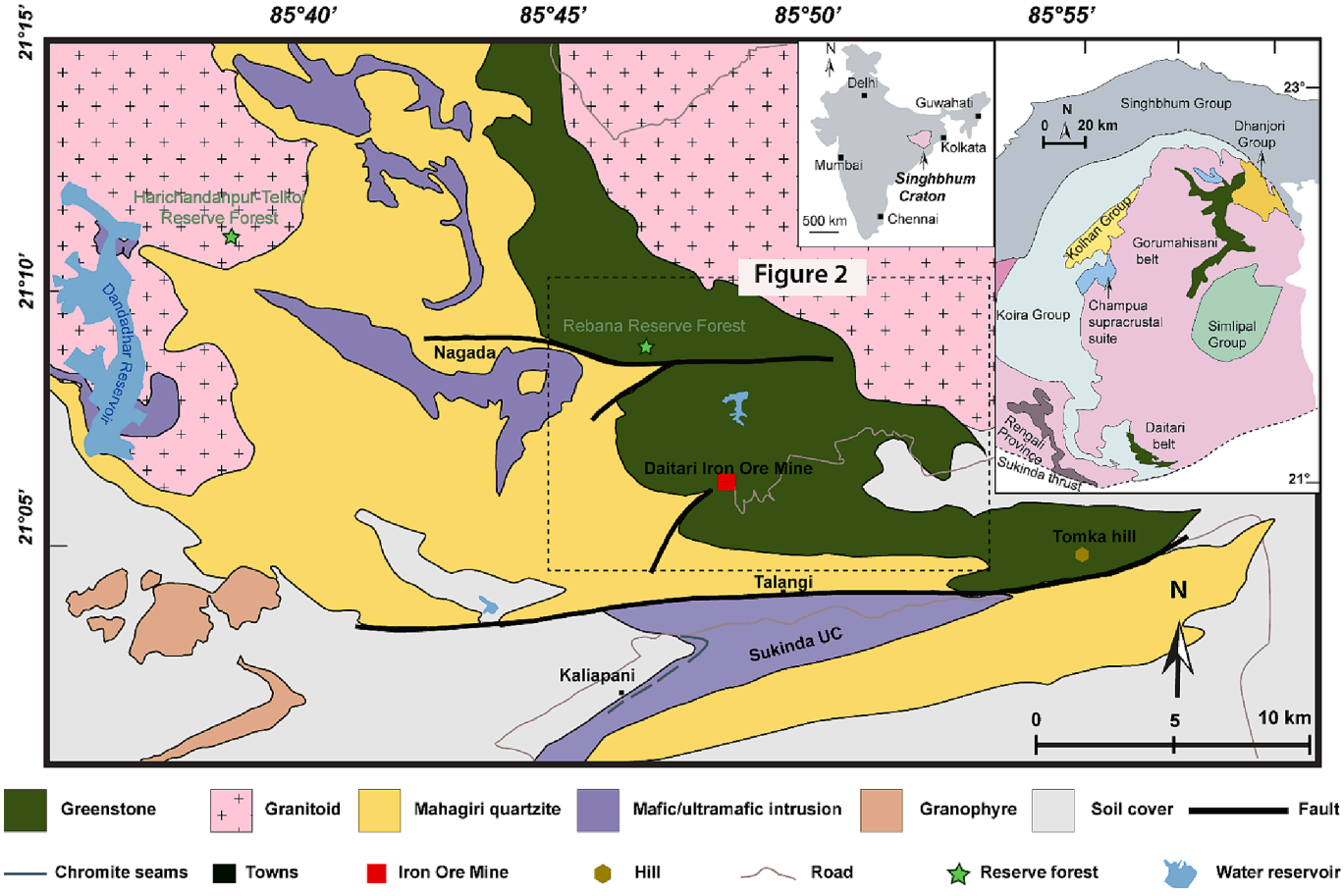


Fig. 1. Geological map of the Daitari Greenstone Belt, Singhbhum Craton, India. Modified after Prasada Rao et al. (1964).

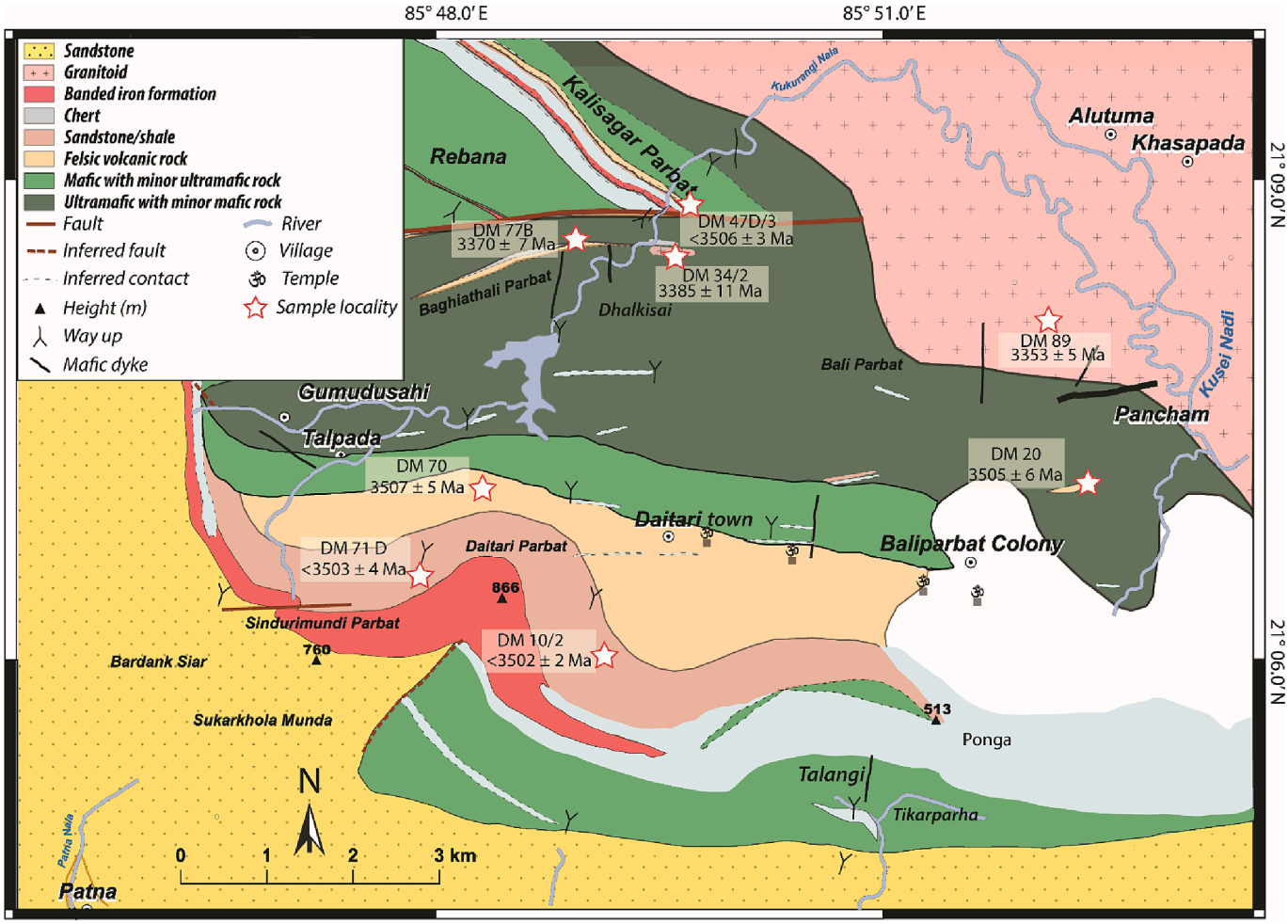


Fig. 2. Geological map of the central portion of Daitari Greenstone Belt (modified after Jodder, 2021). Note star symbols in the map represent sample localities with U-Pb zircon age data.

Mukhopadhyay et al., 2012). Acharya (2002) provided a detailed structural evolutionary history of the DGB. Deformation produced steeply dipping strata with stratigraphic younging largely towards the SSW. Stratification and way up is evident in spinifex-textured komatiite flows, pillowed basalts, cross-laminated sedimentary units and graded beds in the greenstone sequence (Jodder, 2021). The unconformably overlying Mahagiri sedimentary sequence (<3.0 Ga old) preserves excellent sedimentary structures, such as ripple laminations and cross-bedding. The greenstone sequence can be sub-divided into five major lithostratigraphic formations named after mountain ranges and villages, where the volcano-sedimentary rocks are best exposed (Jodder 2021; Fig. 3):

The Kalisagar Formation is the stratigraphically lowest unit of the Daitari belt and consists of a sub-marine ultramafic/mafic volcanic succession (~3 km thick) with minor interbedded chert units. The lower portion of the Kalisagar Formation is intruded by granodiorites to the northeast of the DGB (Fig. 4a). The volcanic rocks include variably deformed massive and pillow basalts (Fig. 4b), talc-carbonate schists, and tremolite-actinolite schists, although spinifex-textured komatiitic flow units are preserved in places. Volcanic rocks are intensely carbonated and silicified where overlain by bedded chert units. Rare quartz-muscovite schists were observed in the field, occurring as thin discontinuous units intercalated with mafic/ultramafic schist.

The ~ 1.5 km thick Talpada Formation sharply overlies the Kalisagar Formation. It consists of dacitic to rhyodacitic rocks with some minor interbedded chert units. Agglomerates to volcanic breccias that preserve primary blocks or bombs embedded within a tuffaceous matrix are common (Fig. 4c). Bedded chert horizons are common towards the upper part of the Talpada Formation and are associated with black chert veins cutting volcanic rocks beneath. Mukhopadhyay et al. (2008) provided a U–Pb age of c. 3507 ± 2 Ma for the dacitic rocks of the Talpada Formation. These authors suggested an island arc affinity for the dacites.

The Sindurimundi Formation is nearly 500 m thick and erosively overlies the felsic volcaniclastic rocks of the Talpada Formation. It is mainly characterised by clastic sedimentary rocks (high– to low–density turbidity current deposits, Fig. 4d) with minor interlayered pillow basalts. Subordinate chert units are interlayered towards the upper part of the stratigraphy. The succession is broadly upward fining with inversely to normally graded conglomerates near the base, graded beds of medium-grained sandstone in the middle part, and finely laminated siltstone, shale, and minor chert horizons near the top.

Orthochemical sedimentary rocks of the Tomka Formation (~700 m thick; Fig. 4d-e) are made up of banded black and white chert (Fig. 4d), and banded iron formation (Fig. 4e). Along the eastern stretches of the DGB, the iron-formation laterally grades into banded chert. The lower part of the Tomka Formation is in sharp contact with the underlying Sindurimundi Formation. The iron formation locally hosts high-grade iron ore mined by Orissa Mining Corporation. Mining activity in the Daitari-Tomka area initiated during the 1960′s (Acharya, 2002).

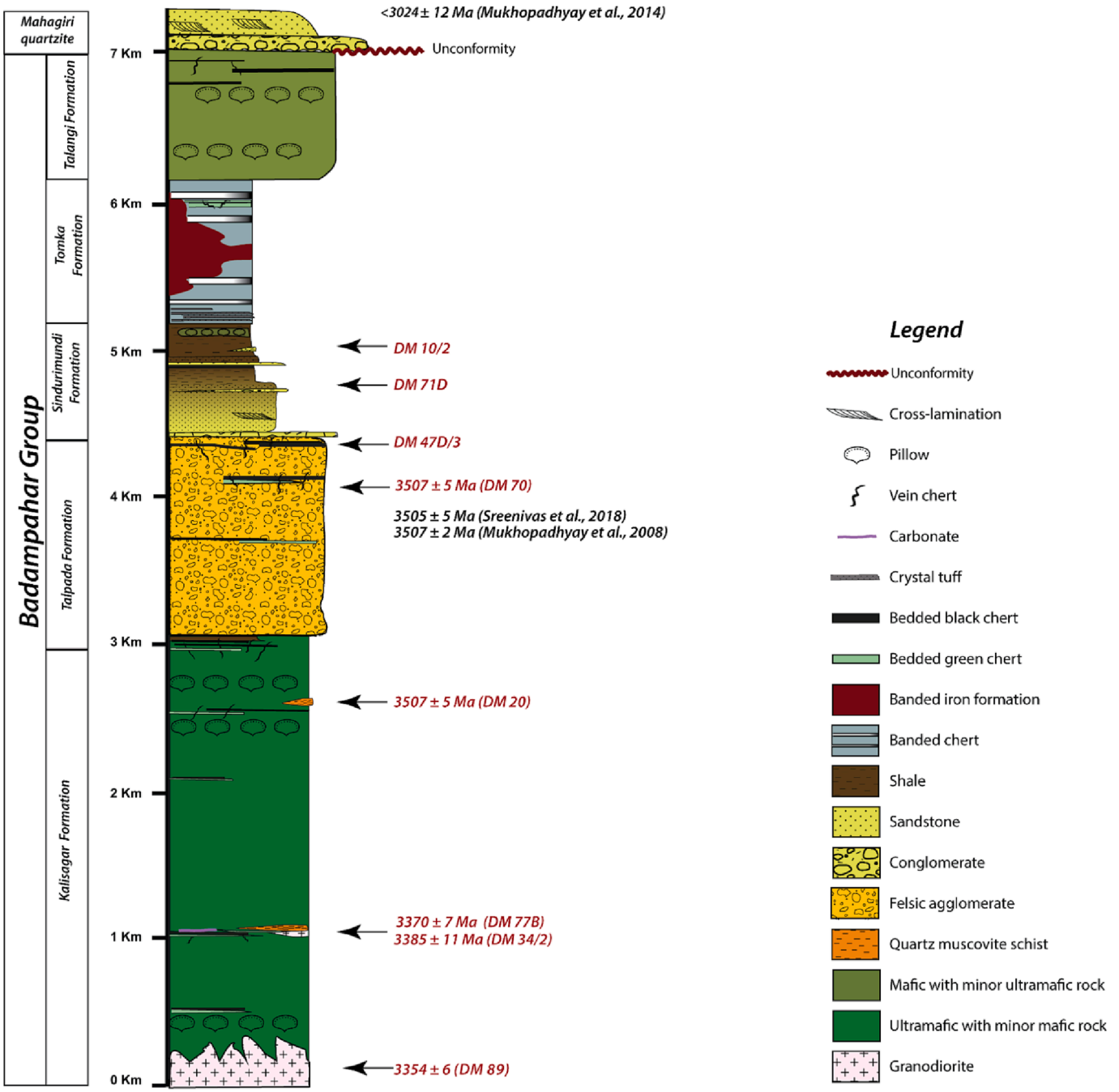


Fig. 3. Stratigraphic column of the Badampahar Group of the Daitari belt (modified from Jodder, 2021) and geochronological information for igneous samples.

The Talangi Formation is marked by a sharp contact with the Tomka Formation and by an unconformable contact relationship with the overlying Mahagiri siliciclastic rocks. The Talangi Formation is a nearly 1 km thick suite of pillowed and massive basalts, spinifex-textured komatiitic basalts and thin interlayered chert units, which indicate a sub-aquatic setting.

3. Sampling and methodology

We studied a variety of igneous and clastic sedimentary rocks mainly for the purpose of age dating in order to resolve the stratigraphy of the volcano-sedimentary rocks exposed in the DGB. These include quartz-muscovite schists of unknown parentage, a granodiorite and trondhjemite, a felsic volcaniclastic rock, two greywacke samples and a phyllite. In addition to age dating, we also provide elemental composition and Lu-Hf zircon isotope systematics of selected samples to provide first-hand information on their bulk-rock geochemistry and crust-mantle evolution signatures.

3.1. Whole-rock major oxide and trace element analyses

Fresh material of four igneous samples was pulverized for major and trace-element geochemistry using an agate mill. Major element contents were determined on fusion disks, using a Panalytical MagiX PRO X-ray fluorescence spectrometer housed at the Spectrum Analytical Facility, University of Johannesburg (refer to Siahi et al. 2018 for analytical procedures). Trace element analyses were done at the School of Geosciences, University of the Witwatersrand, using a Perkin Elmer Sciex

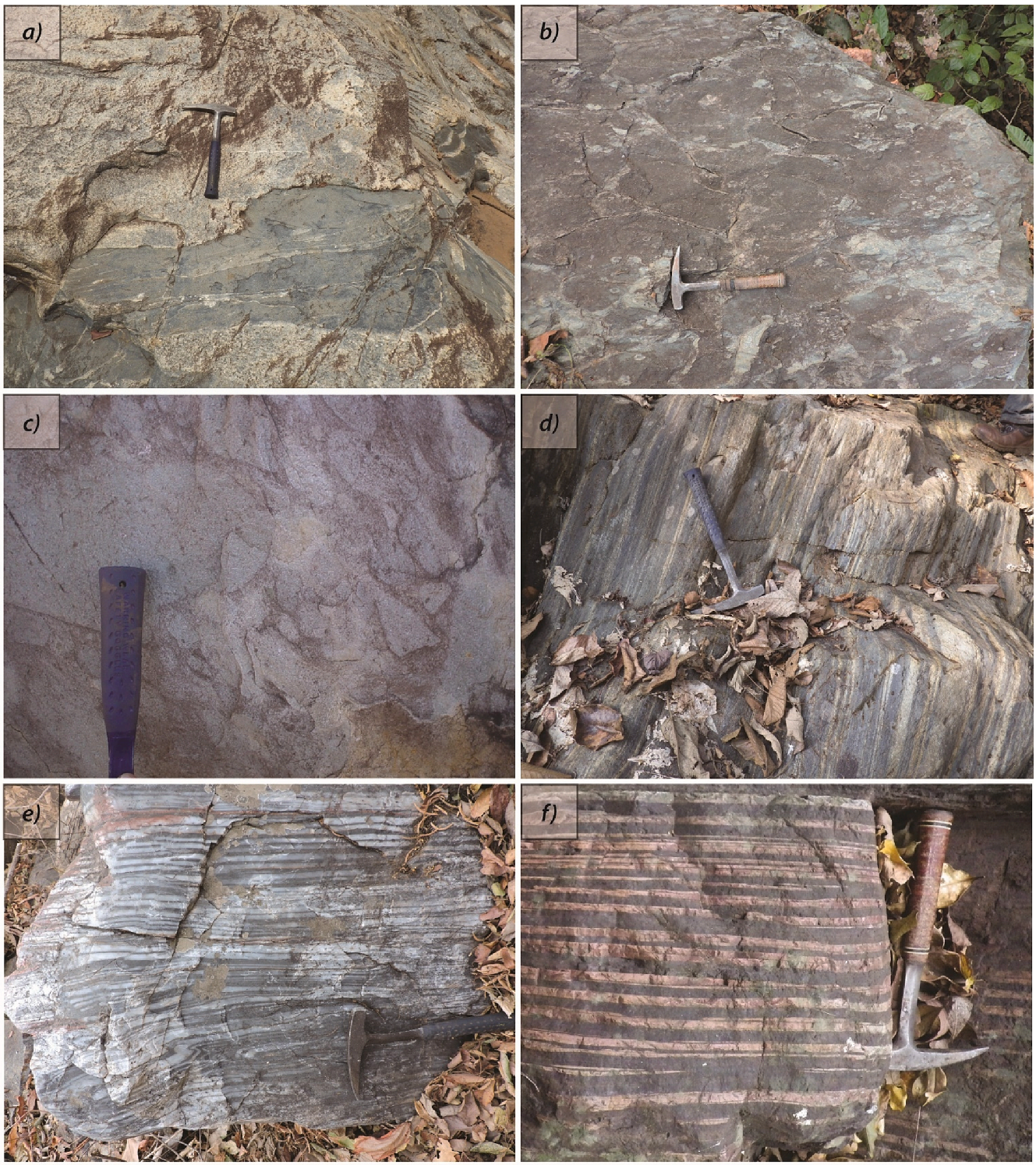


Fig. 4. a) Granodiorite with greenstone xenoliths intrusive into the Kalisagar Formation. b) Pillow basalt, Kalisagar Formation. c) Clast-supported blocks and bombs embedded in a tuffaceous matrix, Talpada Formation. d) Thin, normally graded beds within the turbidite sequence of the Sindurimundi Formation. e) Banded chert, Tomka Formation. f) Banded Iron Formation, Tomka Formation.

ELAN DRC-e Inductively Coupled Plasma-Mass Spectrometer, against primary standard solutions and validated against certified standard rock materials. Details of the analytical procedures can be found in Wilson (2019).

3.2. Zircon U-Pb and Hf analyses

Zircon U–Pb analysis of igneous rocks was performed by SHRIMP II, Beijing SHRIMP Center, Chinese Academy of Geological Sciences, China (see Supplementary material S1). Detrital zircon grains recovered from clastic sedimentary rocks were analysed for U-Pb and Lu-Hf using the LA-ICP-MS facility at the University of Johannesburg, South Africa (see

Supplementary material S1 for details). Zircon crystals and detrital zircon grains were separated using standard techniques of panning and magnetic separation. Individual zircon crystals and detrital zircon grains were hand-picked and mounted on epoxy resin discs, which were polished to expose the internal parts of zircon crystals. Prior to analysis, cathodoluminescence (CL) imaging of the zircons was undertaken to reveal internal textures and growth stages. Analytical procedure, and reference material information are provided in the Supplementary material (S1).

4. Results

4.1. Geochemistry

Results of major and trace-element analyses are presented in Supplementary file S2. Chondrite-normalized REE and primitive mantle-normalized diagrams are shown in Fig. 5a-b. The dacite sample (DM 70) and quartz muscovite schist (DM 77B) have SiO_2 contents consistent with dacite–rhyodacite (72 wt.% and 76 wt.%; Supplementary material S2) of the DGB as reported by Mukhopadhyay et al. (2012). Both samples have high K_2O (i.e., 4.4 wt.% and 5.6 wt.% respectively) and low Na_2O ($\leq$0.1 wt.%) contents. Previous studies from the Daitari and Gorumahisani belts have suggested removal of Na associated with hydrothermal alteration (Mukhopadhyay et al., 2012; Jodder et al., 2021). Sample DM 34/2 (trondhjemite) has a SiO_2 content of 73.5 wt.%, a Na_2O concentration of 5.2 wt.% and a K_2O content of 2.2 wt.%.

A chondrite-normalized rare earth element (REE) plot (Fig. 5a) shows enriched light rare earth elements (LREE) similar to felsic igneous rocks reported previously from the Daitari and Gorumahisani greenstone sequences, with moderate ΣREE contents (42–83 ppm) and moderately fractionated HREE patterns (Gd_N/Yb_N = 5.7–1.7). Zr contents (61 to 110 ppm) are low to moderate when compared to dacitic rocks described by Mukhopadhyay et al. (2008, 2012). In particular, Sr values for felsic igneous rocks (i.e., DM 70 and DM 77B) are lower than most dacitic rocks previously reported from the DGB (Mukhopadhyay et al., 2012), which is indicative of feldspar alteration as evident by low Na_2O contents in these samples. In a primitive mantle-normalized multi-element plot (Fig. 5b) almost all samples show negative anomalies for Sr, P and Ti and a broad negative Nb–Ta anomaly almost identical to felsic igneous rock reported from Gorumahisani belt (Jodder et al., 2021). A consistency in trace element behaviour is noted amongst quartz-muscovite schist (DM 77B), trondhjemite (DM 34/2) and granodiorite (DM 89), when compared to dacite (DM 70). The latter shows a slightly higher concentrations of HREE when compared to the abovementioned felsic igneous rocks (Fig. 5a-b).

4.2. Zircon geochronology

4.2.1. Zircon internal structures

Cathodoluminescence images show that igneous samples preserve zircon with euhedral, prismatic outline and magmatic zoning with some zircon crystals exhibiting patchy and/or disturbed magmatic zoning. In

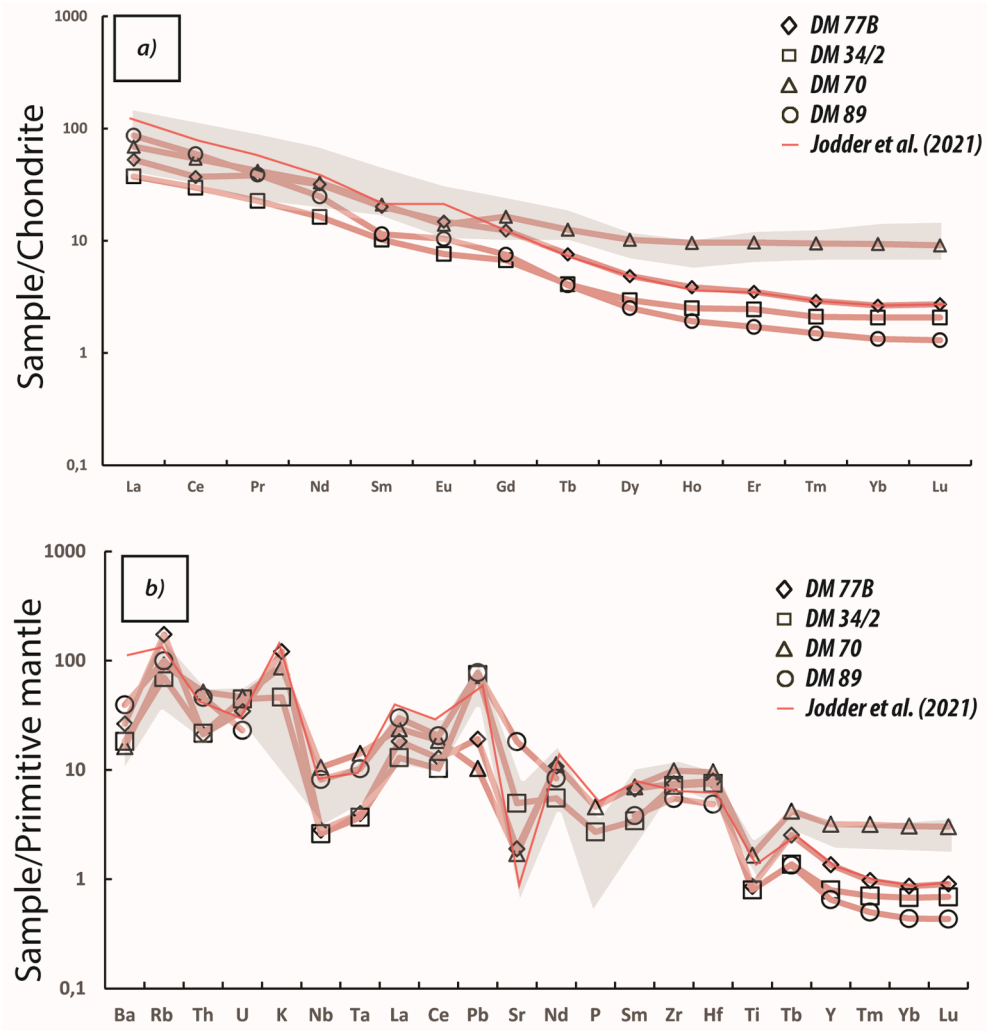


Fig. 5. a) Chondrite-normalized trace element plot of felsic igneous rocks from the Daitari belt (Sun and McDonough, 1985). b) Primitive mantle-normalized trace element plot of felsic igneous rocks from the Daitari belt (McDonough and Sun, 1995). Note trace element data of dacite samples described by Mukhopadhyay et al. (2012) is shown in grey shaded area and trace element data of felsic volcaniclastic sample GUD-3 from the Gorumahisani belt (Jodder et al., 2021) represented by a thin red line. (For interpretation of the references to color in this figure legend, the reader is referred to the web version of this article.)

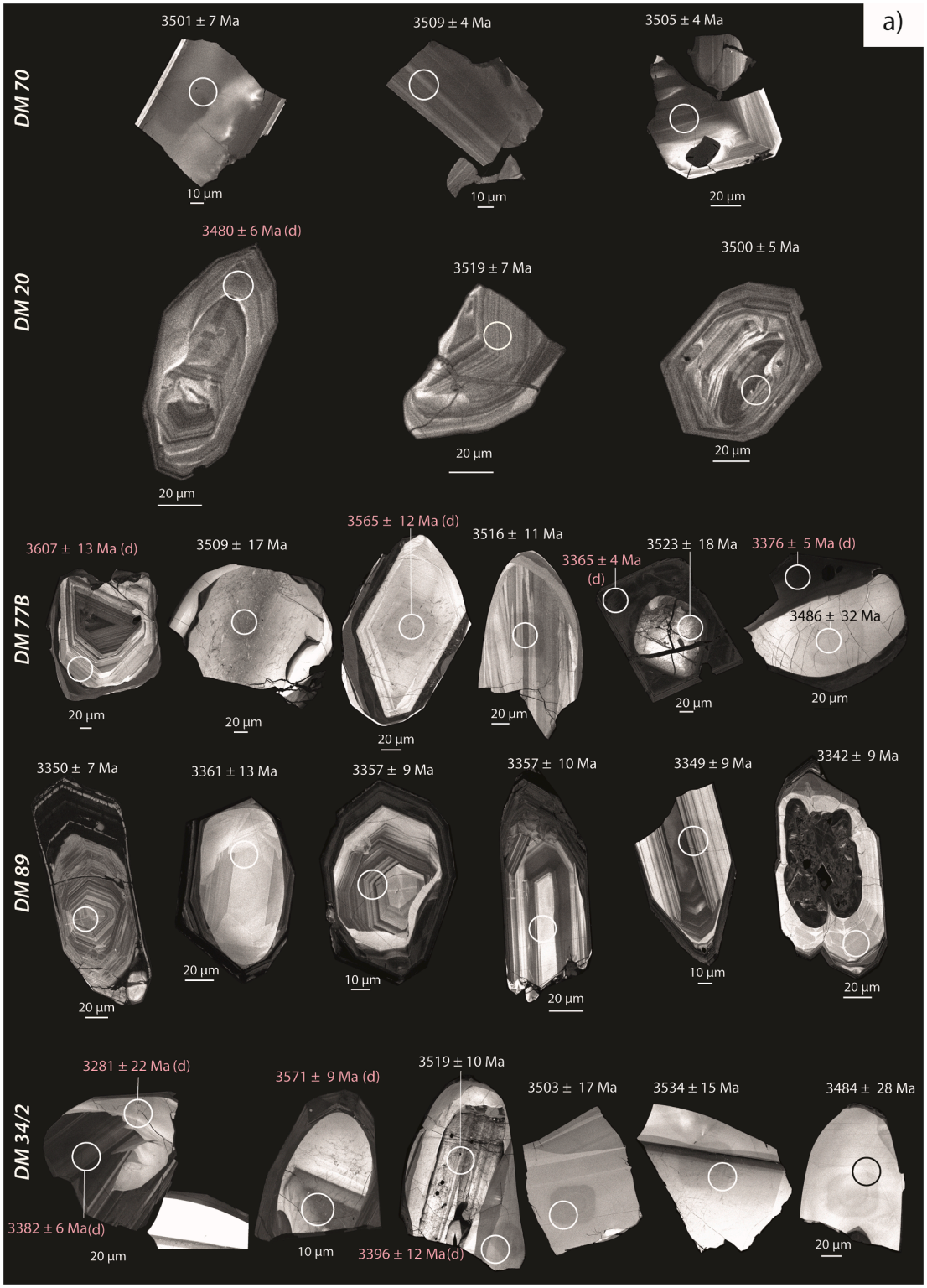


Fig. 6. a) Representative CL images of zircon grains from samples DM 70, DM 20, DM 77B, DM 89 and DM 34/2. Note Zircon U-Pb data indicated in pink color is a discordant datapoint. b) Representative CL images of zircon grains from samples DM 10/2, DM 71D, and DM 47D/3. Note Hf spot analyses were conducted on U-Pb spots . (For interpretation of the references to color in this figure legend, the reader is referred to the web version of this article.)

some zircon crystals, the primary magmatic growth/oscillatory zoning has been wholly erased. Samples DM 34/2, DM 77B and DM 89 preserve trace for older cores (See Fig. 6a), whereas metamict zircons are rare. Some zircon crystals show low luminescent rims, of which most were too narrow to analyse but a few of these rims analysed provided discordant ages. On the other hand, detrital zircon grains (i.e., ~50 and ≤ 200 µm along long axis, Fig. 6b) form a homogeneous population of angular to sub-angular, long- to short-prismatic, euhedral grains. The detrital zircon grains preserve magmatic parallel banding, oscillatory zoning under cathodoluminescence and are free of any visible cores. Few



Fig. 6. (*continued*).

grains, especially in sample DM 10/2, preserve sub-angular to sub-rounded grain shapes that suggest short transportation from the source. Metamict zircon grains were absent and no significant difference was noted in terms of luminescence between central to marginal portions. (Fig. 6b).

4.2.2. *Kalisagar Formation*

A quartz-muscovite schist with abundant quartz phenocrysts (DM 20) was collected from the upper part of the Kalisagar Formation (Fig. 2). The schist is ≥ 2 m in thickness but poorly exposed and interlayered with chlorite schist. Twenty-two analyses were carried out on 22 zircon crystals. No visible core–rim structures could be discerned. Four near-concordant zircon crystals provided concordant results with a weighted mean $^{207}Pb/^{206}Pb$ age of 3505 ± 6 Ma (MSWD = 2.1; Fig. 7a, refer Table 1 and for details see Supplementary file S3).

A sample of trondhjemite (DM 34/2) intrusive into the Kalisagar Formation was collected downstream along Kukurangi Nala (Fig. 2). Sixteen U-Pb analyses were performed on thirteen zircon crystals and yielded three age populations of 3577 ± 53 Ma (i.e., weighted mean of 3 analyses), 3510 ± 9 Ma (i.e., weighted mean of 7 analyses; Fig. 7b, refer Table 1 and Supplementary material S3) and 3385 ± 11 Ma (e.g., weighted mean of 2 analyses; Fig. 7b). The two older age populations are reported from the core regions of some zircon crystals. Because of the clearly intrusive nature of the trondhjemite, we interpret the older population as xenocrysts within a younger magmatic rock, the crystallization age of which is interpreted here at 3385 ± 11 Ma.

From a similar stratigraphic interval as the trondhjemite, a quartz-muscovite schist (DM 77B) interlayered with mafic schist was sampled near the Baghiathali mountain range (Fig. 2). A total of 19 analyses were done on 14 zircon crystals, some showing evidence for older cores (Fig. 7c). Ten analyses fell within a population with a $^{207}Pb/^{206}Pb$ date of 3499 ± 8 Ma (MSWD = 1.2; Supplementary material S3) and three analyses provided a mean $^{207}Pb/^{206}Pb$ date of 3548 ± 9 (MSWD = 1.2). These two slightly older populations are treated as xenocrystic in origin as a younger zircon yield provided a mean $^{207}Pb/^{206}Pb$ date of 3370 ± 7 Ma (n = 3; MSWD = 2.7). The latter is interpreted here as the age of emplacement of the schist precursor, which is coeval in age when compared to trondhjemite sample DM 34/2. Therefore, based on the

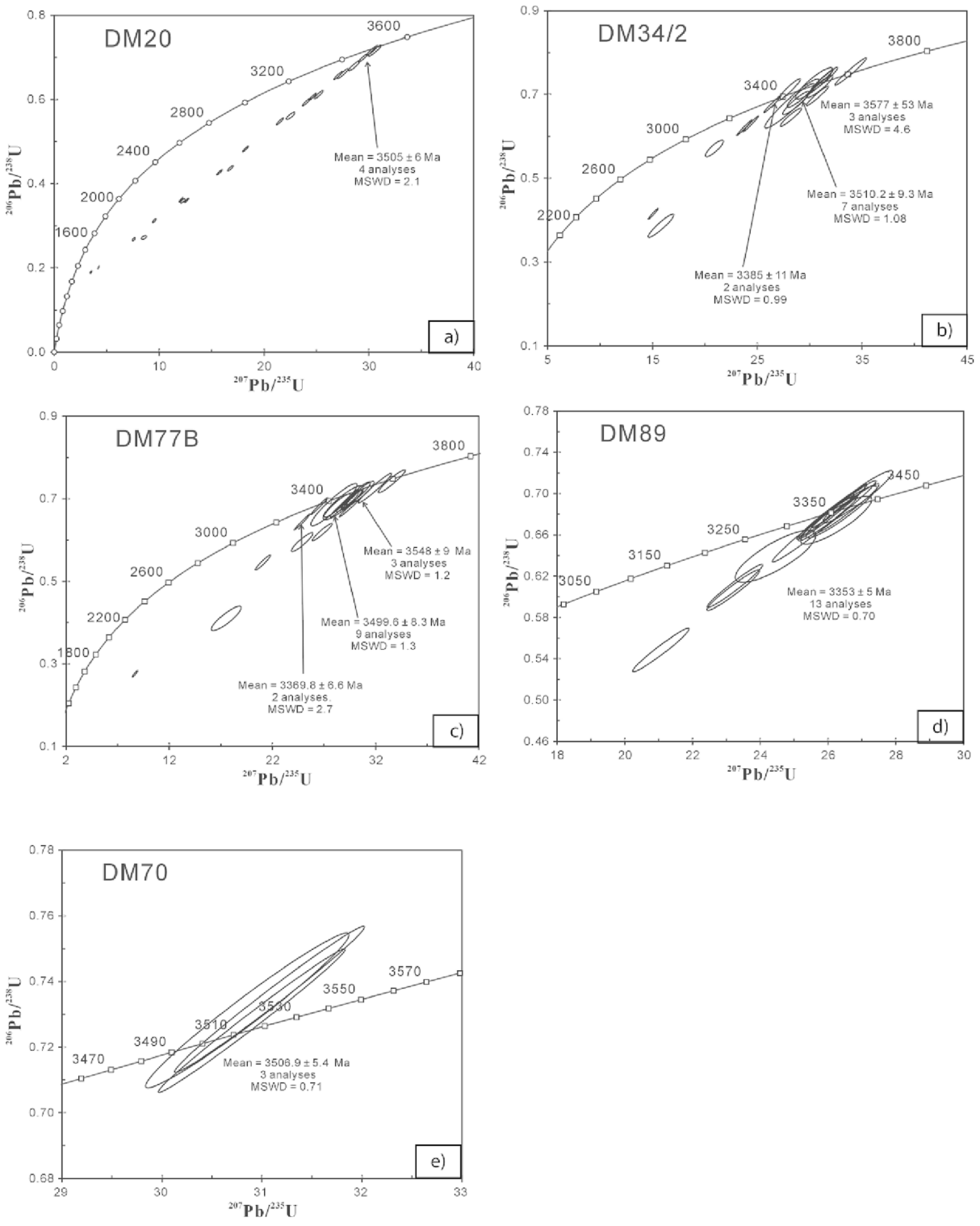


Fig. 7. a-f) Concordia diagrams for U-Pb SHRIMP analyses (Supplementary material S3). Note age ellipses for each analysis are defined by 1-sigma errors in $^{207}Pb/^{235}U$, $^{206}Pb/^{238}U$ and $^{207}Pb/^{206}Pb$. a) Quartz muscovite schist (DM 20). b) Trondjhemite (DM 34/2). **c)** Quartz muscovite schist (DM 77B). d) Granodiorite (DM 89). e) Dacite (DM 70).

identical U-Pb zircon age dates and similar stratigraphic positioning of these studied samples, we interpret DM 77B as a deformed trondhjemite sill intrusive within mafic rocks of the Kalisagar Formation.

A granodiorite (DM 89) was collected from a well-exposed pavement near a streambed section along Pancham River (Fig. 2), which is several kilometres east of its intrusive contact with the greenstones of the Kalisagar Formation. Many zircon crystals contain CL-dark rims that were not analysed in this study. Thirteen zircon crystals were analysed for U-Pb dating that provided a weighted mean $^{207}Pb/^{206}Pb$ date of 3353 ± 5 Ma (MSWD = 0.70; Fig. 7d, Supplementary material S3), which we interpret as the crystallization age of the granodiorite.

4.2.3. *Talpada Formation*

One felsic volcaniclastic rock (DM 70) was collected from the upper

Table 1
Summary of the different samples used in this study from the Daitari belt, Singhbhum Craton, India.

Sample	Description	Latitude and Longitude	Zircon Th/U	Weighted Average age data ($^{207}Pb/^{206}Pb$)
DM 77B (quartz-muscovite schist)	Qz + Ser + Ms + Fe-Ti Ox	21°08′34.7″N, 85°48′29.6″E	0.01–0.81	Mag; 3370 ± 7 Ma (MSWD = 2.7, N = 2) Xe: 3500 ± 8 Ma (MSWD = 1.3, N = 9), 3548 ± 9 Ma (MSWD = 1.2, N = 3)
DM 20 (quartz-muscovite schist)	Qz + Ser + Ms + Fe-Ti Ox ± Chl	21°07′06.0″N, 85°52′11.6″E	0.5–0.9	Mag:3506 ± 6 Ma (MSWD = 2.1, N = 4)
DM 70 (Dacite)	Qz + Ser ± Chl + Fe-Ti Ox	21°06′53.4″N, 85°47′33.0″E	0.8–1.3	Mag: 3507 ± 7 Ma (MSWD = 0.71, N = 3)
DM 89 (Granodiorite)	Qz + Pl + Ser + Chl + Fe-Ti Ox	21°07′16.0″N, 85°53′14.0″E	0.4–0.7	Mag: 3353 ± 5 Ma (MSWD = 0.70, N = 13)
DM 34/2 (Trondhjemite)	Qz + Pl + Fe-Ti Ox + Sul	21°08′29.7″N, 85°49′19.4″E		Mag: 3385 ± 11 Ma (MSWD = 0.99, N = 2), Xe: 3577 ± 53 (MSWD = 4.6, N = 3), 3510 ± 9 Ma (MSWD = 1.08, N = 7)
DM 10/2 (Greywacke)	Qz + Prl + Ser + Rt + CM + Chl	21°07′16.0″N, 85°53′14.0″E	0.4–0.8	Det: 3502 ± 2 Ma (MSWD = 2.0, N = 46)
DM 47D/3 (Phyllite)	Qz + Rt + Ser + CM + Fe-Ti Ox	21°08′47.4″N, 85°49′32.4″E	0.6–1	Det: 3506 ± 3.0 Ma (MSWD = 8.6, N = 41), Det: 3520 ± 4 Ma (MSWD = 0.33, N = 5)
DM 71D (Greywacke)	Qtz + Prl + Ser + Rt + CM + Chl	21°06′45.5″N, 85°47′51.7″E	0.3–0.9	Det: 3503 ± 4 Ma (MSWD = 1.9, N = 28) Det: 3523 ± 11 Ma (MSWD = 0.061, N = 4)

Qtz- quartz, Pl- plagioclase, Ms-muscovite, Ser-sericite, Ox-Oxide, Chl- chlorite, Tr- tourmaline, Sul- sulfides, Prl-Pyrophyllite, Rt- Rutile, CM- Carbonaceous matter, Xe- Xenocrysts, Mag: Magmatic, Det: Detrital. Note Th/U ratios shown here are from concordant zircon only. Mineral abbreviations after Whitney and Evans (2010).

part of the Talpada Formation near the contact with the Sindurimundi Formation turbidite sequence (Fig. 7e). Only three zircon crystals, showing well-developed oscillatory zoning, were recovered during separation. Three analyses were conducted on these zircon crystals and provided concordant U-Pb age data, with a weighted mean $^{207}Pb/^{206}Pb$ date of 3507 ± 5 Ma (refer Supplementary material S3), which we interpret as the crystallization age of this felsic volcanic rock.

4.2.4. *Sindurimundi Formation*

Three samples were analysed from the turbidite sequence of the Sindurimundi Formation. Sample DM 47D/3 was collected from an outcrop downstream along Kukurangi Nala (i.e., north of the Rebana fault, Fig. 2). DM 71D and DM 10/2 were collected within the turbidite sequence near the Talpada valley stream section and close to the contact with the iron formation near Daitari Parbat respectively (Fig. 2). Analytical procedure, and reference material information are provided in the Supplementary material S4.

Forty-nine spot analyses were performed on forty-six zircon grains recovered from silicified phyllite (DM 47D/3). Forty-one zircon grains with very similar ratios (Fig. 8a, see Supplementary material S4), yielded a weighted $^{207}Pb/^{206}Pb$ mean date of 3506 ± 3 Ma (MSWD = 8.6 and 95 % confidence). Five grains provided a mean $^{207}Pb/^{206}Pb$ date of 3520 ± 4 Ma (MSWD = 0.33 and 95 % confidence) and are interpreted to represent a slightly older zircon population (Fig. 8b, see Supplementary material S4 Table 1).

Thirty–nine spot analyses on thirty–six detrital zircon grains from a greywacke (DM 71D) were undertaken. $^{207}Pb/^{206}Pb$ dates of twenty-eight zircon grains are all concordant with very similar ratios, yielding a weighted $^{207}Pb/^{206}Pb$ mean age of 3503 ± 4 Ma (MSWD = 1.9 and 95 % confidence; Fig. 8c; see Supplementary material S4 Table 2). Four slightly older zircon grains provided a mean $^{207}Pb/^{206}Pb$ age of 3523 ± 11 Ma (MSWD = 0.061 and 95 % confidence see Fig. 8d) that reflect an older population cluster.

Fifty-two zircon grains from sample DM 10/2 (greywacke) were analysed for U–Pb dating. Few zircon grains are marked by lead loss and lie on a discordia in the concordia diagram (Fig. 8e, see Supplementary file S4 Table 3). $^{207}Pb/^{206}Pb$ dates of forty-six zircon grains are all concordant with very similar ratios (Fig. 8e) yielding a weighted mean $^{207}Pb/^{206}Pb$ age of 3502 ± 2 Ma (MSWD = 2.0 and 95 % confidence).

4.3. *Lu-Hf analysis of detrital zircon grains*

Lu-Hf analyses were conducted on concordant detrital zircon grains recovered from sedimentary rocks of the Sindurimundi Formation. The results are reported in an $\varepsilon Hf_{(t)}$ vs age diagram (Fig. 9), with chondritic uniform reservoir (CHUR) parameters of Bouvier et al. (2008; $^{176}Lu/^{177}Hf$ = 0.0336; $^{176}Hf/^{177}Hf$ = 0.282785) and depleted mantle (DM) evolution of Griffin et al. (2000;$^{176}Lu/^{177}Hf$ = 0.0384), assuming a linear evolution from c. 4.5 Ga onwards. Samples used in this study were DM 71D and DM 10/2, which contain the same population of ~ 3.5 Ga zircons as the felsic igneous rocks of the underlying Talpada Formation. In order to determine their Hf-evolution, we assigned a uniform age of 3510 Ma to all zircon grains. Lu-Hf analyses of twenty concordant zircons were performed directly on top of the U-Pb spots. The zircon grains analysed show $\varepsilon Hf_{(t)}$ values between −1.1 to 1.6 and initial $^{176}Hf/^{177}Hf$ value that fluctuate from 0.280474 to 0.280537, while $^{176}Lu/^{177}Hf$ ratios yield values between 0.0822×10^{-2} to 0.1917×10^{-2} (Supplementary material S4 Tables 4-5).

5. Discussion

Recent U-Pb zircon studies from the Archaean record of the Singhbhum Craton of India revealed Eoarchaean and Hadean detrital zircon grains within sandstones and/or stream sediments as well as xenocrysts within tonalitic gneisses (Chaudhuri et al., 2018; Miller et al., 2018; Sreenivas et al., 2019, Ranjan et al., 2020; Bhattacharjee et al., 2021). However, rocks of Eoarchaean age have so far not been found in the Singhbhum craton. Preservation of rocks older than ~ 3.5 Ga is rare, and this holds true specifically for low-grade supracrustal rock assemblages. The Palaeoarchaean Badampahar Group of the Daitari greenstone belt provide first-hand information on ancient crustal and surface processes 3.5 Ga ago.

5.1. *Geochronological evolution of the Daitari greenstone belt*

The oldest volcano-sedimentary strata of the DGB are represented by ultramafic and mafic submarine lava plain deposits of the Kalisagar Formation (Figs. 2-3). Quartz-muscovite schist (DM 20) infolded with the mafic schists provided an age of 3505 ± 6 Ma, which is identical to the zircon age of 3507 ± 2 Ma (Mukhopadhyay et al., 2008) and 3507 ± 6 Ma (this study) of the Talpada Formation, which overlies the Kalisagar Formation. We therefore interpret the quartz muscovite schist as a deformed felsic sill within the Kalisagar Formation, likely representing a sub-volcanic intrusion as part of the feeder system to the Talpada Formation volcanic succession. This precise SHRIMP U-Pb age provides a minimum age for the ultramafic/mafic volcanic rocks of the Kalisagar Formation. The age of the felsic volcaniclastic rock (DM 70) from the upper part of the Talpada Formation is indistinguishable from

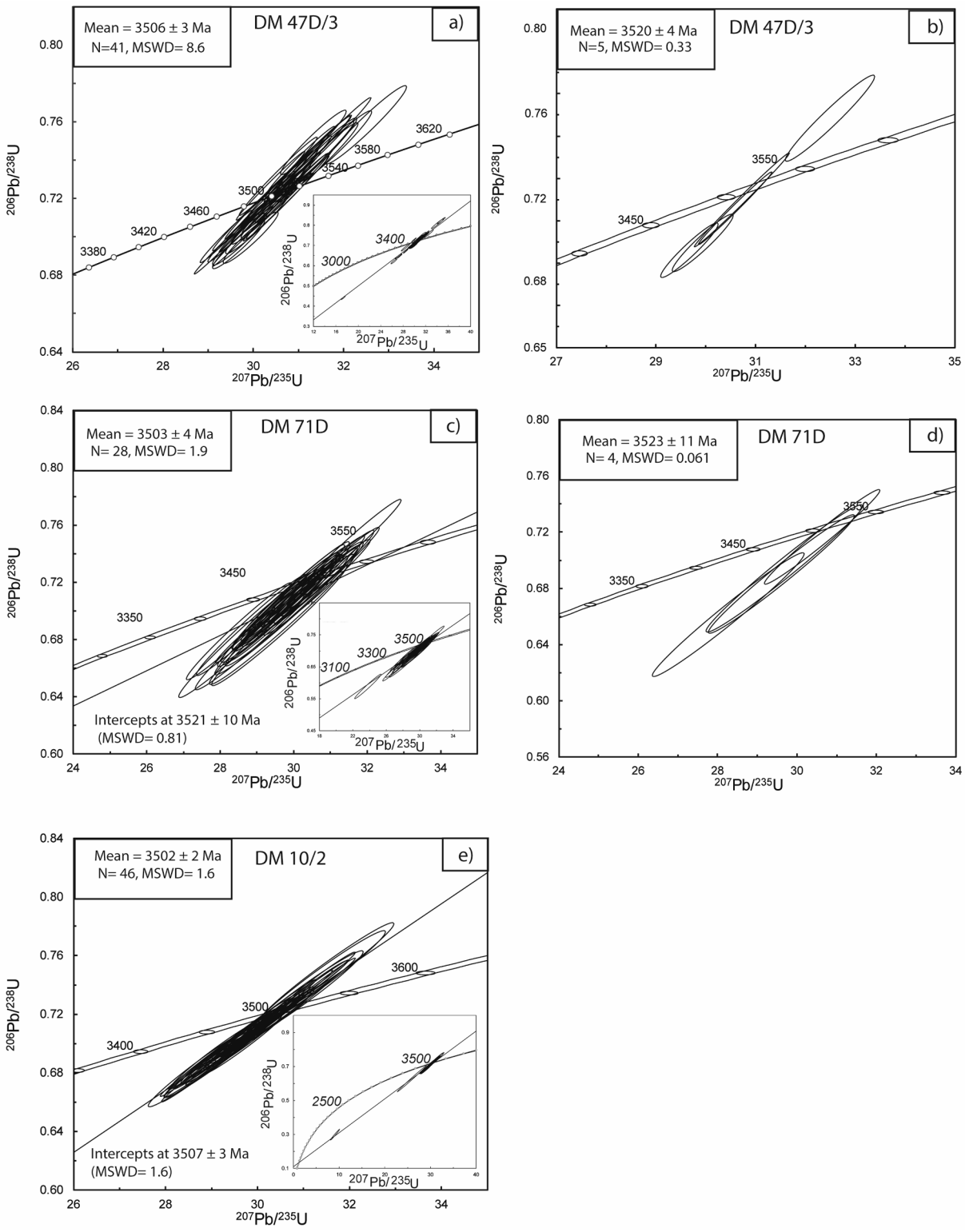


Fig. 8. a-f) Concordia diagrams for U-Pb- LA-ICP-MS analyses (Supplementary material S4) of sedimentary rocks. Note age ellipses for each analysis are defined by 1-sigma errors in $^{207}Pb/^{235}U$, $^{206}Pb/^{238}U$ and $^{207}Pb/^{206}Pb$. a) Phyllite (DM 47D/3) b) Older age cluster with $^{207}Pb/^{206}Pb$ mean age of 3520 ± 4 Ma within sample DM 47 D/3. c) Greywacke (DM 71D) d) Older zircon population is reported from sample DM 71D by 4 concordant zircon grains with U-Pb $^{207}Pb/^{206}Pb$ mean age of 3523 ± 11 Ma. e) Greywacke (DM 10/2).

previously reported U-Pb zircon ages from these rocks (Mukhopadhyay et al., 2008; Sreenivas et al., 2019), which further confirms the ancient age of felsic volcanism in the Daitari area.

The detrital zircon U-Pb ages of the youngest population from the Sindurimundi Formation yielded results of ~ 3505 Ma from DM 10/2 (i.e., 3502 ± 2 Ma), DM 71D (i.e., 3503 ± 4 Ma), and DM 47D/3 (3506 ± 3 Ma) that are indistinguishable to the felsic volcaniclastic rocks of the Talpada Formation dated at 3507 ± 2 Ma (Mukhopadhyay et al., 2008). In this study we report a maximum age of deposition for the clastic suite of rocks of the Sindurimundi Formation of 3502 ± 2 Ma. Thus, the

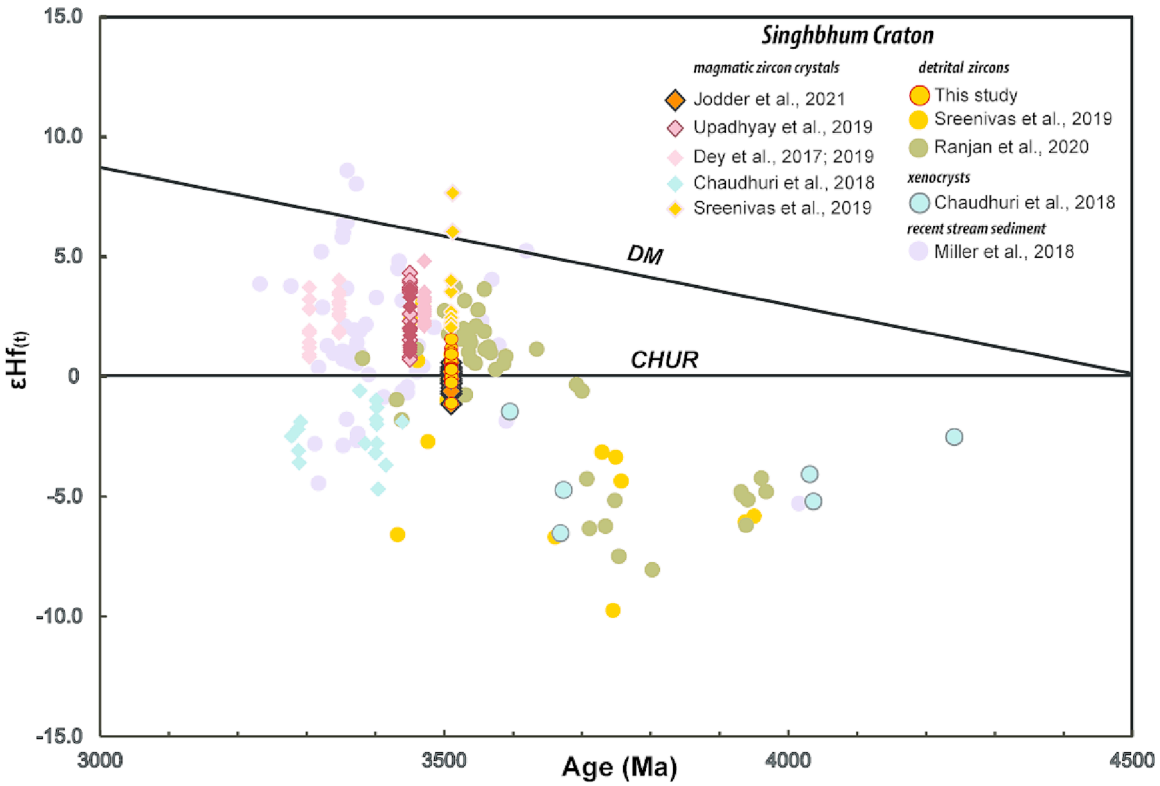


Fig. 9. Plot showing the $\varepsilon Hf_{(t)}$ values vs U-Pb ages of magmatic zircon crystals and sedimentary zircon grains of the Singhbhum Craton.

detrital zircon age presented here is representative of the dominant felsic magmatic event in the Daitari belt and further affirms a predominant source from the weathering and erosion of felsic volcanic rocks, which resulted in the deposition of turbidites of the Sindurimundi Formation.

The detrital zircon ages from the sedimentary sequence of the Sindurimundi Formation provide further insights into the magmatic history of the Talpada Formation. The dominant detrital age population is 3505 ± 5 Ma and a slightly older population is dated at c. 3520 Ma. The former is identical to the felsic volcanic rocks of the Talpada Formation dated so far (Mukhopadhay et al., 2008; Sreenivas et al., 2019; this study) and can be regarded as its source. The older age population of c. 3520 Ma may have been derived from erosion of a yet undated, stratigraphically slightly older felsic volcanic unit. It is also possible that the older detrital zircon population represents xenocrystic zircon crystals entrained within the felsic volcanic rock dated at c. 3505 ± 5 Ma (refer Fig. 8b, d). The latter has been suggested for ~ 3530 Ma zircon crystals in 3510 ± 3 Ma felsic volcanic rocks of the Gorumahisani belt (Jodder et al., 2021). In either case, multi-phase felsic magmatism between 3.50 and 3.53 Ga is indicated for the Singhbhum Craton, and from c. 3502 Ma to 3520 Ma in the DGB, which is reflected in the detrital zircon record of the Sindurimundi Formation.

Based on geochemical proxies Mukhopadhyay et al. (2012) suggested that felsic volcanism in the DGB is linked to arc magmatism along a convergent plate boundary. They further proposed the Sukinda ultramafic complex to be genetically related to the greenstones and referred to the basalt-dacite succession (our Kalisagar and Talpada formations) as a bimodal sequence. By lumping all these rock types together with the overlying BIF, an evolutionary model of an extending oceanic arc–forearc in an oceanic supra–subduction zone geodynamic setting was proposed. However, there is neither a bimodal suite of volcanic rocks nor do the Sukinda ultramafic rocks represent part of an ophiolite. The mafic volcanic rocks and intercalated cherts of the uppermost Kalisagar Formation are in sharp contact with the overlying felsic volcanic rocks of the Talpada Formation (Jodder, 2021). Nowhere are mafic and felsic rocks intercalated, which would be a prerequisite for a succession to be referred to as bimodal. Moreover, the rocks of the Sukinda Complex represent a layered intrusive igneous complex and are likely much younger than the greenstones (Mondal et al., 2007; Auge et al., 2003; Hofmann et al., 2022).

Following the 3.51 Ga felsic magmatism that gave rise to the Talpada Formation, deposition of a thick clastic turbidite sequence of the Sindurimundi Formation took place. The change from widespread felsic magmatism to deposition of turbidites derived from the erosion of felsic volcanics in the DGB is probably linked to erosion of subaerially emerged volcanic edifices. We propose local provenance as a source for the turbidites of the Sindurimundi Formation, which is based on the predominance of felsic volcanic detritus, prevalence of a detrital zircon population dated at 3.51 Ga and the absence of any extraformational clasts.

Deposition of the orthochemical sedimentary suite of the Tomka Formation took place in a submarine setting. Likewise, pillow basalts and minor interlayered bedded cherts in the Talangi Formation indicate marine conditions as well. Geochronological information related to the Tomka and Talangi formations is lacking due to the absence of suitable material for precise dating. Deposition must have taken place between 3507 ± 6 Ma (i.e., the age of the Talpada Formation; this study) and deposition of the Mahagiri siliciclastic rocks after 3024 ± 12 Ma (Mukhopadhyay et al., 2016). Taking the geological evolution of the Singhbhum craton into account, deposition likely took place prior to ~ 3.28 Ga, the approximate age of regional metamorphism of the Badampahar Group (Hofmann et al., 2022).

Between c. 3.37 Ga and 3.35 Ga, TTG plutons and felsic sills intruded the lower part of the greenstone stratigraphy of the Daitari belt. These intrusions may have fed concomitant felsic volcanism not recorded in Daitari belt but found elsewhere in the Champua greenstone belt remnant (cf. Hofmann et al., 2022). The gneissic fabric of the c. 3.35 Ga old granodiorite indicates emplacement prior to the main phase of deformation of the Daitari belt, the exact timing of which remains to be clarified, but which may have happened at c. 3.28 Ga ago from

observations made elsewhere in the Singhbhum craton (Nelson et al., 2014; Chaudhuri et al., 2018, Pandey et al., 2019).

5.2. Tectonic history of the Daitari greenstone sequence and its co-evolution with the Singhbhum Granitoid Complex

Inherited zircon crystals preserved within felsic sills and granodiorite intrusive into the Kalisagar Formation yielded slightly older ages of 3548 ± 9 Ma and 3577 ± 53 Ma relative to the felsic magmatic event at 3.51 Ga reported from the Talpada Formation. This is indicative of a somewhat older felsic component within the source of the melts. Ages of ca. 3.53 Ga were reported from felsic volcanic rocks of the Gorumahisani Greenstone Belt (GGB) and a TTG to the north of the GGB (Acharyya et al., 2010; Jodder et al., 2021; Mitra et al., 2022). Greenstone belt volcanism and concomitant TTG plutonism thus likely started as early as 3.55 Ga in the Singhbhum Craton (Acharyya et al., 2010; Mitra et al., 2022). This is not surprising, since the Kalisagar Formation must be older than 3.51 Ga, and its substrate remains unknown.

Magmatic ages of c. 3.37 and 3.35 Ga, which are represented by different intrusions into the lower part of the Kalisagar Formation, indicate felsic magmatism in the southern part of the Singhbhum Craton. Previous geochronological studies performed on tonalite-trondhjemite-granodiorite rocks from the northern and central parts of the Singhbhum Craton have provided U-Pb ages that fall into the same range (Chaudhuri et al., 2018; Pandey et al., 2019; Upadhyay et al., 2014, 2019). Granitoids that range from ~ 3.38 Ga to 3.25 Ga have been related to the Singhbhum Suite of the Singhbhum Granitoid Complex (Dey et al., 2017; Hofmann et al., 2022).

The chemical composition of the felsic igneous rocks is broadly similar to those previously described from the DGB and GGB and the TTG's from the Singhbhum Granitoid Complex, (Mukhopadhyay et al., 2012; Mitra et al., 2019). Negative Nb, Ta and Ti anomalies are typical for Archaean TTG and associated volcanic rocks, but their geodynamic setting cannot be constrained from their composition alone. They may have derived from melting of hydrated or silicified mafic rocks in a subduction or oceanic plateau-like setting (e.g., Foley et al., 2000; André et al., 2019), possibly relatively deep in the crust (Martin et al., 1987), or at more shallow crustal levels but subjected to plagioclase and hornblende fractionation (Liou and Guo, 2019; Rollinson, 2021). Nevertheless, REE patterns allow to differentiate the ~ 3.35 Ga intrusive granitoids from the ~ 3.51 Ga volcaniclastic dacite, with the latter being less HREE-depleted. This may be interpreted in two ways, either due to difference in pressures of magma generation or via plagioclase- and amphibole-dominated fractionation combined with variable crystal–liquid unmixing (e.g., Laurent et al., 2020). A discussion of these is however beyond the scope of this paper.

5.3. Lu-Hf systematics of the c. 3.5 Ga zircon record of the Singhbhum Craton indicate juvenile crustal growth

Widespread felsic magmatism and crustal growth in the Singhbhum Craton around c. 3.5 Ga is indicated by the presence of TTG's (~3.53 Ga), felsic volcanic rocks (~3.51 Ga), zircon xenocrysts dated around ~ 3.55 Ga to 3.51 Ga and detrital zircon populations ranging from c. 3.55 to 3.51 Ga (Acharyya et al., 2010; Mukhopadhyay et al., 2008; Sreenivas et al., 2019; Ranjan et al., 2020; Bhattacharjee et al., 2021; Jodder et al., 2021; Frimmel et al., 2022; this study). Hf isotope analyses of igneous zircons from TTG's and granites, ranging between ca. 3.4–3.2 Ga, of the Singhbhum Granitoid Complex have indicated a predominantly juvenile crustal component (Dey et al., 2019; Chaudhuri, 2020; Dey et al., 2020; Vijaya Kumar et al. 2021). Likewise, Hf isotope data of zircon grains dated around c. 3.53 to 3.51 Ga yield near to chondritic $\varepsilon Hf_{(t)}$ values that range from –1.0 to 2.8, which are largely indicative of juvenile contributions during that time (cf. Sreenivas et al., 2019, Ranjan et al. 2020). A Nd-isotope study of Palaeoarchaean TTG also support their juvenile sources (Tait et al., 2011). In favour of this notion, detrital zircon grains from the turbidites of the Sindurimundi Formation have near chondritic $\varepsilon Hf_{(t)}$ values between −1.1 to 1.6. They are similar to the $\varepsilon Hf_{(t)}$ values from 3.51 Ga magmatic zircon crystals of felsic volcanic rocks of the Gorumahisani Greenstone Belt (See Fig. 7c, Jodder et al., 2021).

Sreenivas et al. (2019) reported positive εHf(t) compositions from the c. 3.51 Ga old dacitic rocks of the Daitari belt, in contrast to our chondritic $\varepsilon Hf_{(t)}$ data from reworked zircons eroded from the same dacitic rocks. We note that the data reported by Sreenivas et al. (2019) extend to epsilon Hf values that lie above the Depleted Mantle curve, which may point to analytical problems. These could be related to either peak overlap of ^{176}Yb on ^{176}Hf or assuming too old an age for the analysed zircon domain (cf. Kemp et al., 2019), considering that the U-Pb age pit is generally shallower than the ablation crater for Hf isotope analyses. Alternatively, the preferential dissolution of accessory mineral phases, such as rutile or apatite, may have led to a locally higher $^{176}Hf/^{177}Hf$ in the melt, which could explain the radiogenic Hf values in their 3.51 Ga old zircon crystals (cf. Hammerli and Kemp, 2021).

5.4. Felsic magmatism 3.5 Ga ago from the Singhbhum, Kaapvaal and Pilbara cratons

The Badampahar Group greenstone sequence exposed in the Daitari belt is comparable to the Onverwacht Group of the Barberton Greenstone Belt (BGB) in the Kaapvaal Craton of South Africa and the Warrawoona Group of the East Pilbara Terrane of Western Australia (Byerly et al., 2019; Van Kranendonk et al., 2019) in terms of its age, lithological make-up and degree of preservation. More specifically, felsic volcanic and volcaniclastic rocks interlayered with minor chert horizons of the Talpada Formation in the Daitari belt may find their counterpart in the c. 3.53 Ga Theespruit Formation of the Barberton belt, where felsic volcanic and volcaniclastic rocks, their sheared equivalents, and cherts have been reported (see Fig. 10; Kisters and Anhaeusser, 1995a; Diener, 2004; Diener et al., 2005). Another contemporaneous greenstone sequence with felsic volcanic rocks dated at c. 3.53 Ga occurs in the Toggekry Formation of the Nondweni Greenstone Belt (NGB), southeastern Kaapvaal Craton (refer Fig. 10; Wilson and Versfeld, 1994a; Xie et al., 2012). Felsic volcanic rocks of the Coucal Formation dated at 3515 ± 3 Ma mark the earliest phase of felsic volcanism from the Warrawoona Group of the Pilbara Craton, Australia (Fig. 10; Buick et al., 1995; Green et al., 2000; Smithies et al., 2019).

In all these places, the felsic rocks have experienced deformation and metamorphism and are largely preserved as quartz-sericite schists. Nonetheless, primary textures and structures are well-preserved in areas of low-strain (Wilson and Versfeld, 1994; Buick et al., 1995; Diener, 2004; Diener et al., 2005; Mukhopadhyay et al., 2008; this study). In the Theespruit Formation, felsic agglomerates and conglomerates are common, the latter largely consisting of felsic volcanic clasts and less common banded chert and mafic clasts (Diener, 2004; Hofmann and Harris, 2008). Felsic units from the Coonterunah Group are mostly made up of amygdaloidal dacite, dacitic porphyry, dacitic-rhyolitic breccia, and hyaloclastite (Buick et al., 1995; Green et al., 2000). A common aspect of these felsic volcanic units is the widespread presence of interlayered sedimentary units, which reflect discontinuous eruption and sedimentation during volcanic quiescence (Wilson and Versfeld, 1994a; Buick et al., 1995; Diener, 2004; Green et al., 2000; Mukhopadhyay et al., 2008; this study).

The association of mafic and felsic volcanic units preserved in the greenstones of the Nondweni, Onverwacht and Coonterunah groups have been attributed to bimodal volcanism (Green et al., 2000; Van Kranendonk et al. 2009; Xie et al., 2012). All these units have been deformed considerably, necessitating evaluation of depositional vs tectonic or intrusive origin of bimodality (cf. Barker and Arth, 1976). For example, quartz-muscovite schists intercalated with mafic/ultramafic schists in the Kalisagar Formation represent intrusions, and could only be recognized as such by zircon dating due to strong deformation. As such, the Kalisagar Formation is not a bimodal succession. Tectonic

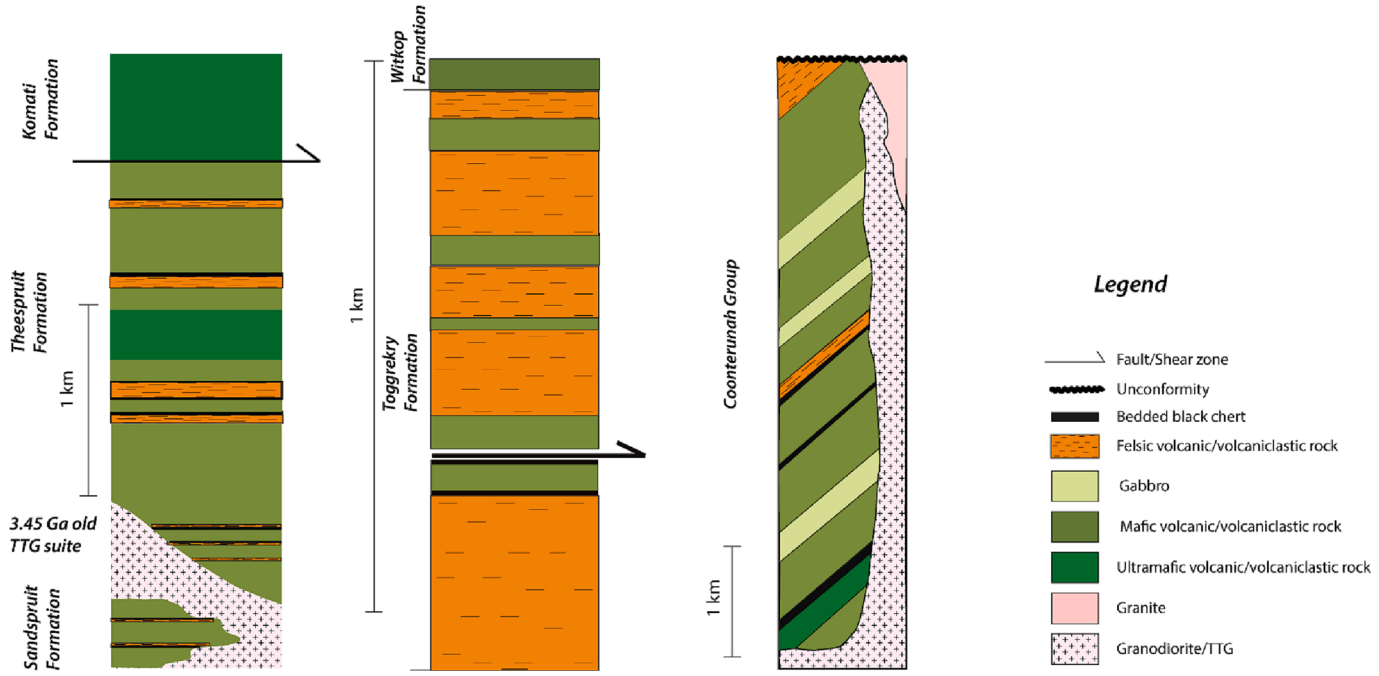


Fig. 10. Stratigraphic columns of the lowermost Onverwacht Group, Nondweni and Coonterunah groups of the Kaapvaal and Pilbara cratons respectively (Figure modified after Viljoen and Viljoen, 1969a; Wilson and Versfeld, 1994a, and Green et al., 2000). (For interpretation of the references to color in this figure legend, the reader is referred to the web version of this article.)

duplication due to thrusting has been reported from the greenstones of the Nondweni belt (e.g., Wilson and Versfeld, 1994a), which could, in principle, cause tectonic interleaving of genetically unrelated mafic and felsic units. However, in most cases described here, felsic rocks occur in the form of volcaniclastic, epiclastic and siliciclastic rocks, necessitating a primary stratigraphic control of bimodality. The clastic nature of some of the felsic volcanic rocks further indicate lateral transport of fragmented material by volcanic and/or sedimentary processes and their deposition into deep-water settings floored by mafic/ultramafic lava flows.

On the basis of geochemical and isotopic studies, different tectonic settings such as volcanic arc-mantle plume interaction, a back-arc basin environment and intracontinental rift have been proposed to explain Archaean bimodal volcanism (cf. Wilson and Versfeld, 1994; Green et al., 2000; Chavagnac; 2004; Furnes et al., 2011; Xie et al., 2012; Agangi et al., 2020). In the Daitari belt, the Talpada Formation consists of felsic volcaniclastic rocks with minor interbedded chert units, very similar in both age and lithological assemblage to those described from other cratons. It however lacks intercalated mafic and ultramafic lava flows, thus not representing a bimodal succession. This may indicate a rather short interval of felsic volcanism, close proximity to felsic volcanic centres and/or a distal setting relative to co-magmatic mafic vents.

Co-existence of felsic volcanic rocks and their intrusive mid-crustal equivalents of TTG's ranging from ~ 3.51 Ga to 3.23 Ga have been documented from the Barberton granitoid-greenstone terrain (Agangi et al., 2018; de Wit et al., 1987 and references therein). Likewise, 3.5 Ga old felsic volcanic rocks exposed in the Daitari and Gorumahisani belts have a coeval TTG equivalent exposed north-east of the Gorumahisani area (see Mukhopadhyay et al., 2008; Acharyya et al., 2010; Jodder et al., 2021; Mitra et al., 2022). In the Pilbara Craton, coeval plutonic equivalents of the Coucal Formation are represented by the 3.53–3.49 Ga Mulgundoona Supersuite (Petersson et al., 2020).

A definite understanding of the generation and/or emplacement mechanisms of felsic volcanic rocks and TTG from the Singhbhum Craton is lacking. Generation of Archaean felsic melts have been a major topic of debate (cf. Willbold et al., 2009; Nebel et al., 2018). Their geochemical analysis have led many authors to argue for subduction processes early on in the Archaean in a plate tectonic regime (cf. Drummond et al., 1990, 1996; Foley et al., 2002; Martin et al., 2014). Others have argued for a stagnant (single)-lid tectonic setting, with episodic melting of the base of oceanic plateau-like crust above zones of mantle upwelling (e.g., Bedard; 2006; Smithies et al., 2009; Bedard et al., 2018). Shallow melting of silicified seafloor volcanics in such a setting can explain the geochemistry of Archaean TTG's (Andre et al., 2019, 2022). It seems clear that different mechanisms may have been able to produce felsic melts in the Palaeoarchaean, giving rise to emplacement of TTG's and their volcanic counterparts. Why such rocks of a narrow age range of 3.51 – 3.53 Ga are found on the Kaapvaal, Pilbara and Singhbhum cratons remains unclear. This may reflect proximity of these terrains as part of a single crustal entity during Palaeoarchaean times, subjected to the same tectonic processes regionally. Alternatively, felsic magmatism at ~ 3.5 Ga was a global process, potentially linked to global mantle upwelling and melting of thick, hydrothermally altered greenstone crust. Another question relates to preservation of 3.5 Ga volcano-sedimentary succession near the base of the Palaeoarchaean supracrustal piles in these cratons, with the lack of much older strata. Further research on the oldest preserved geologic record of these cratons will provide new insights into crustal processes and evolution of ancient continents during the Palaeoarchaean and potentially older times.

6. Conclusions

Ultramafic-mafic volcanic rocks from the Kalisagar Formation, the lowermost preserved part of the Badampahar Group in the Daitari Greenstone Belt, are older than 3.51 Ga, as indicated by the age of an intrusive felsic sill dated at 3505 ± 6 Ma and the age of the overlying felsic volcanic rocks of the Talpada Formation dated at 3507 ± 6 Ma. This event of felsic magmatism is also recorded by TTG's and volcanics in the northeastern part of the Singhbhum Craton. Following felsic volcanism, erosion of the volcanic edifice gave rise to the deposition of turbidity current deposits of the Sindurimundi Formation. The youngest zircon age fraction from the Sindurimundi Formation is indistinguishable to the age of the felsic volcaniclastic rocks of the Talpada

Formation, which acted as the main source of detritus. We suggest the maximum age of deposition of the Sindurimundi Formation to be 3502 ± 2 Ma. Therefore, the detrital zircon data further affirm the importance of the felsic magmatic event around 3.5 Ga in the Daitari belt. Detrital zircon grains dated from the turbidites of the Sindurimundi Formation contain an older age fraction of around 3.53 Ga, which corresponds to a slightly early phase of felsic magmatism in the DGB. Orthochemical sedimentary rocks of the Tomka Formation predominantly indicate sub-marine depositional settings, followed by sub-marine volcanism of the youngest, but yet to be dated Talangi Formation.

Zircon U–Pb age data from a deformed trondhjemite sill (c. 3.37 Ga), which is intrusive into the lower part of the greenstone succession, suggests emplacement of a pre-tectonic suite of TTG (i.e., Champua suite) in the Daitari area. Furthermore, a magmatic zircon age of c. 3.35 Ga obtained from an intrusive granodiorite exposed north of the Daitari belt marks a significant phase of plutonic activity in the Singhbhum Craton, which is now documented from the northern, central and southern parts of the Singhbhum Craton, respectively, forming part of the Singhbhum Granitoid Complex. Xenocrystic zircon populations dated at c. 3.55 within intrusive rocks indicates a slightly earlier phase of felsic magmatism in the Singhbhum Craton, Hf-in-zircon data from the 3.51 Ga volcano-sedimentary rocks record juvenile source contribution with no evidence for reworking of pre-existing heterogenous sources. Finally, evidence for felsic volcanism and/or TTG plutonism around 3.5 Ga is common to all granite–greenstone terrains from the Singhbhum, Kaapvaal and Pilbara cratons.

Declaration of Competing Interest

The authors declare that they have no known competing financial interests or personal relationships that could have appeared to influence the work reported in this paper.

Data availability

Supplementary files

Acknowledgements

The DSI-NRF Centre of Excellence for Integrated Mineral and Energy Resource Analysis (CIMERA) of South Africa is acknowledged for financial support through their funding programme via a Doctoral Fellowship to Jaganmoy Jodder. GENUS Africa is acknowledged for a post-doctoral research fellowship to the first author. Authors would like to thank Spectrum analytical facility, University of Johannesburg and Earth Lab, University of Witwatersrand. The LA-MC-ICP-MS at the Department of Geology, University of Johannesburg, was funded by NRF NEP grant # 93208. JJ is grateful to Odisha Mining Corporation Limited (OMC) for their assistance and help during the various field seasons in the Daitari area. Discussions with Andrea Agangi and Christophe Balouard have improved this manuscript. JJ thanks Dora Paprika for sample mount preparation and Marylou Vines for assistance with QGIS. The first author dedicates this article to his uncle *late Prasanta Mandal*, who inspired JJ to visit ancient mountains. We appreciate insightful comments by two anonymous reviewers and efficient editorial handling by Prof. Wilson Teixeira.

Appendix A. Supplementary data

Supplementary data to this article can be found online at https://doi.org/10.1016/j.precamres.2023.106997.

References

Acharya, S., 2002. The Daiteri-Tomka Basin: its structural and stratigraphic evolution and genesis of associated iron ores. Indian J. Geol. 74, 49–81.

Acharyya, S.K., 1993. Greenstones from Singhbhum craton, their Archaean character, oceanic crustal affinity and tectonics. Proc. Nat. Acad. Sci. India Sec. A 63, 211–222.

Acharyya, S.K., Gupta, A., Orihashi, Y., 2010. New U-Pb zircon ages from Palaeo-Mesoarchaean TTG gneisses of the Singhbhum Craton, eastern India. Geochemical Journal. 44, 81–88.

Adhikari, A., Mukherjee, S., Vadlamani, R., 2021. A plume-mantle interaction model for the petrogenesis of komatiite-komatiitic basalt-basalt-basaltic andesite volcanism from the Paleoarchean (3.57–3.31 Ga) Iron Ore Group greenstone belts, Singhbhum craton, India: Constraints from trace element geochemistry and SmNd geochronology. Lithos 106315.

Agangi, A., Hofmann, A., Elburg, A.M., 2018. A review of Palaeoarchaean felsic volcanism in the eastern Kaapvaal craton: Linking plutonic and volcanic records. Geoscience Frontiers. 9, 667–688.

Agangi, A., Hofmann, A., Hegner, E., Xie, H., Teschner, C., Slabunov, A., Svetov, S.A., 2020. The Mesoarchaean Dominion Group and the onset of intracontinental volcanism on the Kaapvaal craton–geological, geochemical and temporal constraints. Gondwana Research 84, 131–150.

André, L., Abraham, K., Hofmann, A., Monin, L., Kleinhanns, I.C., Foley, S., 2019. Early continental crust generated by reworking of basalts variably silicified by seawater. Nature Geoscience 12 (9), 769–773.

André, L., Monin, L., Hofmann, A., 2022. The origin of early continental crust: New clues from coupling Ge/Si ratios with silicon isotopes. Earth and Planetary Science Letters 582, 117415.

Anhaeusser, C.R., 2014. Archaean greenstone belts and associated granitic rocks–A review. Journal of African Earth Sciences 100, 684–732.

Augé, T., Cocherie, A., Genna, A., Amstrong, R., Guerrot, C., Mukherjee, M.M., Patra, R. N., 2003. Age of the Baula PGE mineralization (Orissa, India) and its implications concerning the Singhbhum Archean Nucleus. Precambrian Res. 121, 85–101.

Barker, F., Arth, J.G., 1976. Generation of trondhjemitic-tonalitic liquids and Archean bimodal trondhjemite-basalt suites. Geology 4, 596–600.

Bauer, A.M., Reimink, J.R., Chacko, T., Foley, B.J., Shirey, S.B., Pearson, D.G., 2020. Hafnium isotopes in zircons document the gradual onset of mobile-lid tectonics. Geochemical Perspectives Letters 14, 1–6.

Bédard, J.H., 2006. A catalytic delamination-driven model for coupled genesis of Archaean crust and sub-continental lithospheric mantle. Geochimica et cosmochimica acta 70 (5), 1188–1214.

Bhattacharjee, S., Mulder, J.A., Roy, S., Chowdhury, P., Cawood, P.A., Nebel, O., 2021. Unravelling depositional setting, age and provenance of the Simlipal volcano-sedimentary complex, Singhbhum craton: Evidence for Hadean crust and Mesoarchean marginal marine sedimentation. Precambrian. Research. 354, 106038.

Bouvier, A., Vervoort, J.D., Patchett, P.J., 2008. The Lu–Hf and Sm–Nd isotopic composition of CHUR: constraints from unequilibrated chondrites and implications for the bulk composition of terrestrial planets. Earth Planetary Science Letters. 273 (1–2), 48–57.

Buick, R., Thornett, J.R., McNaughton, N.J., Smith, J.B., Barley, M.E., Savage, M., 1995. Record of emergent continental crust~ 3.5 billion years ago in the Pilbara Craton of Australia. Nature 375 (6532), 574–577.

Byerly, R., Gary., Lowe., R, Donald., and Heubeck, Christoph. 2019. Geologic Evolution of the Barberton Greenstone Belt—A Unique Record of Crustal Development, Surface Processes, and Early Life 3.55–3.20 Ga. *Earth's Oldest Rocks (Second Edition). Earth's Oldest Rocks (Second Edition). In: Developments in Precambrian Geology. Elsevier*. Pp: 569-613.

Chaudhuri, T., 2020. A review of Hadean to Neoarchean crust generation in the Singhbhum Craton, India and possible connection with Pilbara Craton, Australia: The geochronological perspective. Earth-Science Reviews 202, 103085.

Chaudhuri, T., Wan, Y., Mazumder, R., Ma, M., Liu, D., 2018. Evidence of enriched, Hadean mantle reservoir from 4.2-4.0 Ga zircon xenocrysts from Paleoarchean TTGs of the Singhbhum Craton, Eastern India. Scientific reports. 8 (1), 1–12.

Chavagnac, V., 2004. A geochemical and Nd isotopic study of Barberton komatiites (South Africa): implication for the Archean mantle. Lithos 75 (3–4), 253–281.

Chowdhury, P., Mulder, J.A., Cawood, P.A., Bhattacharjee, S., Roy, S., Wainwright, A.N., Nebel, O., Mukherjee, S., 2021. Magmatic thickening of crust in non–plate tectonic settings initiated the subaerial rise of Earth's first continents 3.3 to 3.2 billion years ago. Proc. Natl. Acad. Sci. 118.

de Wit, M.J., Armstrong, R., Hart, R.J., Wilson, A.H., 1987. Felsic igneous rocks within the 3.3-to 3.5-Ga Barberton greenstone belt: High crustal level equivalents of the surrounding tonalite-trondhjemite terrain, emplaced during thrusting. Tectonics 6 (5), 529–549.

Dey, S., Mitra, A., Nandy, J., Mondal, S., Topno, A., Liu, Y., and Zong, K. 2019. Chapter 30: Early crustal evolution as recorded in the granitoids of the Singhbhum and Western Dharwar Cratons. *Earth's Oldest Rocks (Second Edition). In: Developments in Precambrian Geology. Elsevier.* 741–792.

Dey, S., Topno, A., Liu, Y., Zong, K., 2017. Generation and evolution of Palaeoarchaean continental crust in the central part of the Singhbhum craton, eastern India. Precambrian Research. 298, 268–291.

Dey, S., Nayak, S.K., Mitra, A., Zong, K., Liu, Y., 2020. Mechanism of Paleoarchean continental crust formation as archived in granitoids from the northern part of Singhbhum Craton, eastern India. Geol. Soc. Lond. Spec. Publ. 489, 189–214.

Dhuime, B.C.J., Hawkesworth, P.A., Cawood, C.D., 2012. A Change in the Geodynamics of Continental Growth 3 Billion Years Ago. Science 335, 1334–1336.

Diener, J.F., 2004. The tectono-metamorphic evolution of the Theespruit Formation in the Tjakastad schist belt and surrounding areas of the Barberton Greenstone Belt, South Africa. University of Stellenbosch, Stellenbosch. Doctoral dissertation.

Drummond, M.S., Defant, M.J., Kepezhinskas, P.K., 1996. Petrogenesis of slab-derived trondhjemite-tonalite-dacite/adakitemagmas. Trans. R. Soc. Edinburgh-Earth Sci. 87, 205–215.

Foley, S.F., Barth, M.G., Jenner, G.A., 2000. Rutile/melt partition coefficients for trace elements and an assessment of the influence of rutile on the trace element characteristics of subduction zone magmas. Geochimica et Cosmochimica Acta. 64, 933–938.
Foley, S., Tiepolo, M., Vannucci, R., 2002. Growth of early continental crust controlled by melting of amphibolite in subduction zones. Nature 417 (6891), 837–840.
Frimmel, H.E., Chakravarti, R., Basei, M.A.S., 2022. Detrital zircon ages from Archaean conglomerates in the Singhbhum Craton, eastern India: implications on economic Au-U potential. Miner Deposita 57, 1499–1514.
Furnes, H., de Wit, M.J., Robins, B., Sandstå, N.R., 2011. Volcanic evolution of the upper Onverwacht Suite, Barberton Greenstone Belt, South Africa. Precambrian Research 186, 28–50.
Greber, N.D., Dauphas, N., Bekker, A., Ptáček, M.P., Bindeman, I.N., Hofmann, A., 2017. Titanium isotopic evidence for felsic crust and plate tectonics 3.5 billion years ago. Science 357 (6357), 1271–1274.
Green, M.G., Sylvester, P.J., Buick, R., 2000. Growth and recycling of early Archaean continental crust: geochemical evidence from the Coonterunah and Warrawoona Groups, Pilbara Craton. Australia. Tectonophysics 322 (1–2), 69–88.
Griffin, W.L., Pearson, N.J., Belousova, E., Jackson, S.E., Van Achterbergh, E., O'Reilly, S.Y., Shee, S.R., 2000. The Hf isotope composition of cratonic mantle: LAM-MC-ICPMS analysis of zircon megacrysts in kimberlites. Geochimica et Cosmochimica Acta. 64, 133–147.
Hammerli, J., Kemp, T.I.S., 2021. Combined Hf and Nd isotope microanalysis of co-existing zircon and REE-rich accessory minerals: High resolution insights into crustal processes. Chemical Geology 581, 120393.
Diener, F., A., J. G. Stevens, A.F.M. Kisters, M. Poujol. Metamorphism and exhumation of the basal parts of the Barberton greenstone belt, South Africa: constraining the rates of Mesoarchaean tectonism Precambrian Research, 143 (1–4) (2005), pp. 87-112.
Hickman, A.H., 1983. Geology of the Pilbara Block and its environs. Western Australia Geological Survey, Bulletin, vol. 127, 268 pp.
Hofmann, A., Bolhar, R., 2007. Carbonaceous cherts in the Barberton greenstone belt and their significance for the study of early life in the Archean record. Astrobiology. 7, 355–388.
Hofmann, A., Harris, C., 2008. Stratiform alteration zones in the Barberton greenstone belt: a window into subseafloor processes 3.5 to 3.3 Ga ago. Chemical Geology. 257, 224–242.
Hofmann, A., Anhaeusser, C.R., Dixon, J., Kröner, A., Saha, L., Wilson, A., Xie, H., 2019. Archaean Granitoid-Greenstone Geology of the Southeastern Part of the Kaapvaal Craton. In: Kröner, A., Hofmann, A. (Eds.), the Archaean Geology of the Kaapvaal Craton, Southern Africa. Springer, Cham, Switzerland, pp. 33–54.
Hofmann, A., Jodder, J., Xie, H., Bolhar, R., Whitehouse, M., Elburg, M., 2022. The Archaean geological history of the Singhbhum Craton, India – a proposal for consistent framework for craton evolution. Earth Science Reviews. 228, 103994.
Homann, M., 2019. Earliest life on earth: evidence from the Barberton Greenstone Belt. South Africa. Earth-Science Reviews 196, 102888.
Iyengar, S.V.P., Murthy, Y.G.K., 1982. The evolution of the Archaean Proterozoic crust in parts of Bihar and Orissa, eastern India. Geol. Surv. India Rec. 112, 1–5.
Jena, B.K., Behra, U.K., 2000. The oldest supracrustal belt from Singhbhum Craton and its possible correlation. Precambrian Crust in eastern and Central India. Proc. UNESCO-IUGS-IGCO, 368. Geol. Surv. India Spec. Publ. 57, 106–121.
Jodder, J., Hofmann, A., Ueckermann, H., 2021. 3.51 Ga old felsic volcanic rocks and carbonaceous cherts from the Gorumahisani Greenstone Belt-Insights into the Palaeoarchaean record of the Singhbhum Craton, India. Precambrian Research 357, 106109.
Jodder, J., 2021. The Geology of the Daitari Greenstone Belt, Singhbhum Craton, India-Insights into Early Life 3.5 Ga Ago. Doctoral dissertation, University of Johannesburg, South Africa.
Kamber, B.S., 2015. The evolving nature of terrestrial crust from the Hadean, through the Archaean, into the Proterozoic. Precambrian Research. 258, 48–82.
Kröner, A., Hoffmann, J.E., Xie, H., Wu, F., Münker, C., Hegner, E., Wong, J., Wan, Y., Liu, D., 2013. Generation of early Archaean felsic greenstone volcanic rocks through crustal melting in the Kaapvaal, craton, southern Africa. Earth and Planetary Science Letters. 381, 188–197.
Kisters, A.F.M., Anhaeusser, C.R., 1995a. The structural signifi cance of the Steynsdorp pluton and anticline within the tectonomagmatic framework of the Barberton Mountain Land. South African Journal of Geology 98, 43–51.
Kemp, A.I., Whitehouse, M.J., Vervoort, J.D., 2019. Deciphering the zircon Hf isotope systematics of Eoarchean gneisses from Greenland: implications for ancient crust-mantle differentiation and Pb isotope controversies. Geochimica et Cosmochimica Acta 250, 76–97.
Kumar, A., Parashuramulu, V., Shankar, R., Besse, J., 2017. Evidence for a Neoarchean LIP in the Singhbhum craton, eastern India: implications to Vaalbara supercontinent. Precambrian Research 292, 163–174.
Laurent, O., Björnsen, J., Wotzlaw, J.F., Bretscher, S., Pimenta Silva, M., Moyen, J.F., Ulmer, P., Bachmann, O., 2020. Earth's earliest granitoids are crystal-rich magma reservoirs tapped by silicic eruptions. Nature Geoscience 13 (2), 163–169.
Liou, P., Guo, J., 2019. Generation of Archaean TTG gneisses through amphibole-dominated fractionation. Journal of Geophysical Research: Solid Earth. 124 (4), 3605–3619.
Martin, H., Moyen, J.-F., Guitreau, M., Blichert-Toft, J., Le Pennec, J.-L., 2014. Why Archaean TTG cannot be generated by MORB melting in subduction zones. Lithos 198, 1–13.
Mazumder, R., Chaudhuri, T., De, S., Bauer, W., Al Hadi, M., Sugitani, K., van Zuilen, M. A., Senda, R., Yamamoto, M., Raju, P.S. and Ohta, T., 2022. Paleoarchean surface processes and volcanism: Insights from the eastern Iron Ore Group, Singhbhum craton, India. *Earth-Science Reviews*, p.104122.
Mazumder, R., Chaudhuri, T., 2021. Paleoarchean terrestrial to shallow marine sedimentation on Singhbhum Craton, eastern India (the Western Iron Ore Group). Precambrian Research 354, 106071.
Miller, S.R., Mueller, P.A., Meert, J.G., Kamenov, G.D., Pivarunas, A.F., Sinha, A.K., Pandit, M.K., 2018. Detrital zircons reveal evidence of Hadean crust in the Singhbhum Craton. India. *The Journal of Geology*. 126 (5), 541–552.
Mitra, A., Dey, S., Zong, K., Liu, Y., Mitra, A., 2019. Building the core of a Paleoarchean continent: evidence from granitoids of Singhbhum Craton, eastern India. Precambrian Research. 335, 105436.
Mitra, A., Dey, S., Das, P., Zong, K., Liu, Y., Mitra, A., Gond, K. A. 2022. Time-space evolution of an ancient continent, a window to crustal evolution: Insight from granitoids of Singhbhum Craton, eastern India. Earth Science Reviews. *In press*.
Mohakul, J.P., Bhutia, S.P., 2015. Regional structural analysis and reinterpretation in the Bonai-Keonjhar Belt, Singhbhum craton: Implication for revision of the lithostratigraphic succession. J. Geol. Soc. India 85, 26–36.
Mondal, S.K., Frei, R., Ripley, E.M., 2007. Os isotope systematics of mesoarchean chromitite-PGE deposits in the Singhbhum Craton (India): Implications for the evolution of lithospheric mantle. Chemical Geology 244 (3–4), 391–408.
Mukhopadhyay, J., Beukes, N.J., Armstrong, R.A., Zimmermann, U., Ghosh, G., Medda, R.A., 2008. Dating the Oldest Greenstone in India: A 3.51-Ga Precise U-Pb SHRIMP zircon age for dacitic lava of the Southern Iron Ore Group, Singhbhum Craton. The Journal of Geology. 116, 449–461.
Mukhopadhyay, J., Ghosh, G., Zimmermann, U., Guha, S., Mukherjee, T., 2012. A 3.51 Ga bimodal volcanics-BIF-ultramafic succession from Singhbhum Craton: implications for Palaeoarchaean geodynamic processes from the oldest greenstone succession of the Indian subcontinent. Geological Journal. 47, 284–311.
Mukhopadhyay, D., Matin, A., 2020. The Architecture and Evolution of the Singhbhum Craton. Episodes 43 (1), 19–50.
Mukhopadhyay, J., Mishra, B., Chakrabarti, K., De, S., Ghosh, G., 2016. Uraniferous paleoplacers of the Mesoarchean Mahagiri Quartzite, Singhbhum craton, India: Depositional controls, nature and source of> 3.0 Ga detrital uraninites. Ore Geology Reviews 72, 1290–1306.
Mulder, J.A.O., Nebel, N.J., Gardiner, P.A., Cawood, A.N., Wainwright, T.J., 2021. Ivanic Crustal rejuvenation stabilised Earth's first cratons. Nat. Commun. 12, 1–7.
Murty, V.N., Acharya, S., 1975. Lithostratigraphy of the Precambrian rocks around Koira, Sundergarh district. Orissa. J. Geol. Soc. India 16, 55–68.
Naeraa, T., Schersten, A., Rosing, M.T., Kemp, A.I.S., Hoffmann, J.E., Kokfelt, T.F., Whitehouse, M.J., 2012. Hafnium isotope evidence for a transition in the dynamics of continental growth 3.2 Gyr ago. Nature. 485, 627–630.
Nebel, O., Capitanio, F.A., Moyen, J.-F., Weinberg, R.F., Clos, F., Nebel-Jacobsen, Y.J., Cawood, P.A., 2018. When crust comes of age: on the chemical evolution of Archaean, felsic continental crust by crustal drip tectonics. Philos. Trans. R. Soc. Math. Phys. Eng. Sci. 376, 20180103.
Nelson, D.R., Bhattacharya, H.N., Thern, E.R., Altermann, W., 2014. Geochemical and ion-microprobe U-Pb zircon constraints on the Archaean evolution of Singhbhum Craton, eastern India. Precambrian Res. 255, 412–432.
Olierook, H.K., Clark, C., Reddy, S.M., Mazumder, R., Jourdan, F., Evans, N.J., 2019. Evolution of the Singhbhum Craton and supracrustal provinces from age, isotopic and chemical constraints. Earth-Science Reviews. 193, 237–259.
Pandey, O.P., Mezger, K., Ranjan, S., Upadhyay, D., Villa, I.M., Nägler, T.F., Vollstaedt, H., 2019. Genesis of the Singhbhum Craton, eastern India; implications for Archean crust-mantle evolution of the Earth. Chemical Geology 512, 85–106.
Petersson, A., Kemp, A.I.S., Gray, C.M., and Whitehouse, M.J., 2020. Formation of early Archean granite–greenstone terranes from a globally chondritic mantle: insights from igneous rocks of the Pilbara Craton, Western Australia: Chemical Geology, v. 551, p. 1–25, article no. 119757, doi:10.1016/j. chemgeo.2020.119757.
Prasada Rao, G.H.S.V., Murty, Y.G.K., Deekshitulu, M.N., 1964. Stratigraphic relations of Precambrian iron formations and associated sedimentary sequences in parts of Keonjhar, Cuttack, Dhenkanal and Sundergarh districts of Orissa, India. Proc. 22nd Intl. Geol. Cong. India, Sec. X, pp. 72–87.
Ranjan, S., Upadhyay, D., Prusetha, K.L., Nanda, J.K., 2020. Detrital zircon evidence for change in geodynamic regime of continental crust formation 3.7–3.6 billion years ago. Earth Planetary Science Letters. 538, 1–9.
Reimink, J., Chacko, T., Stern, R., et al., 2014. Earth's earliest evolved crust generated in an Iceland-like setting. Nature Geosci 7, 529–533.
Rollinson, H., 2021. Do all Archaean TTG rock compositions represent former melts? Precambrian Research 367, 106448.
Saha, A.K., 1994. Crustal evolution of Singhbhum North Orissa, Eastern India. Memoir of Geological Society of India 27, 341p.
Saha, D., Bachhar, P., Deb, G.K., Patranabis-Deb, S., Banerjee, A., 2021. Tectonic evolution of the Paleoarchean to Mesoarchean Badampahar-Gorumahisani belt, Singhbhum craton, India-Implications for coexisting arc and plume signatures in a granite-greenstone terrain. Precambrian Res. 357, 106094.
Siahi, M., Hofmann, A., Master, S., Wilson, A., Mayr, C., 2018. Trace element and stable (C, O) and radiogenic (Sr) isotope geochemistry of stromatolitic carbonate rocks of the Mesoarchaean Pongola Supergroup: implications for seawater composition. Chemical Geology. 476, 389–406.
Smithies, R.H., Champion, D.C., Van Kranendonk, M.J., 2009. Formation of Paleoarchean continental crust through infracrustal melting of enriched basalt. Earth Planet. Sci. Lett. 281, 298–306.
Smithies, R.H., Champion, D., Van Kranendonk, M.J., 2019. The oldest wellpreserved felsic volcanic rocks on Earth: Geochemical clues to the early evolution of the Pilbara Supergroup and implications for the growth of a Paleoarchean protocontinent. In: Van Kranendonk, M.J., Bennett, C., Hoffmann, J.E. (Eds.), Earth's Oldest Rocks: Amsterdam. Elsevier, pp. 463–486.

Sreenivas, B., Dey, S., Rao, Y.B., Kumar, T.V., Babu, E.V.S.S.K., Williams, I.S., 2019. A new cache of Eoarchaean detrital zircons from the Singhbhum craton, eastern India and constraints on early Earth geodynamics. Geoscience Frontiers. 10 (4), 1359–1370.
Srivastava, R.K., Söderlund, U., Ernst, R.E., Mondal, S.K., Samal, A.K., 2019. Precambrian mafic dyke swarms in the Singhbhum craton (eastern India) and their links with dyke swarms of the eastern Dharwar craton (southern India). Precambrian Research 329, 5–17.
Sugitani, K., 2019. Early Archean (Pre-3.0 Ga) cellularly preserved microfossils and microfossil-like structures from the Pilbara Craton, Western Australia—a review. Earth's oldest rocks 1007–1028.
Tait, J., Zimmermann, U., Miyazaki, T., Presnyakov, S., Chang, Q., Mukhopadhyay, J., Serrgeeve, S., 2011. Possible juvenile Palaeoarchaean TTG magmatism in eastern India and its constraints for the evolution of the Singhbhum Craton. Geol. Mag. 148, 340–347.
Tice, M.M., Lowe, D.R., 2006. The origin of carbonaceous matter in pre-3.0 Ga greenstone terrains: a review and new evidence from the 3.42 Ga Buck Reef Chert. Earth-Science Reviews. 76, 259–300.
Upadhyay, D., Chattopadhyay, S., Kooijman, E., Mezger, K., Berndt, J., 2014. Magmatic and metamorphic history of Paleoarchean tonalite–trondhjemite–granodiorite (TTG) suite from the Singhbhum craton, eastern India. Precambrian Research. 252, 180–190.
Upadhyay, D., Chattopadhyay, S., Mezger, K., 2019. Formation of Paleoarchean-Mesoarchean Na-rich (TTG) and K-rich granitoid crust of the Singhbhum craton, eastern India: constraints from major and trace element geochemistry and Sr-Nd-Hf isotope composition. Precambrian Research. 327, 255–272.
Van Kranendonk, M.J., Smithies, R.H., and. Champion, C.D. 2019. Paleoarchean development of a continental nucleus: the East Pilbara Terrane of the Pilbara Craton, Western Australia. *In Van Kranendonk, M.J., Bennet, V., & Hoffmann, E., eds. Earth's Oldest Rocks 2nd edition. 15:307-337.*.
Van Kranendonk, Kröner, A., Hegner, E., Connelly, J., 2009. Age, lithology and structural evolution of the c. 3.53 Ga Theespruit Formation in the Tjakastad area, southwestern Barberton Greenstone Belt, South Africa, with implications for Archaean tectonics. Chemical Geology 261 (1–2), 115–139.
Vijaya Kumar, T., Bhaskar Rao, Y.J., Babu, E.V.S.S.K., Sreenivas, B., 2021. Journal of the Geological Society of India 97 (10), 1226–1239.
Viljoen, M.J., Viljoen, R.P., 1969a. The geology and geochemistry of the lower ultramafic unit of the Onverwacht Group and a proposed new class of igneous rocks. Geological Society of South Africa Special Publication 2, 55–86.
Viljoen, R.P., Viljoen, M.J., 1969b. The geological and geochemical significance of the upper formations of the Onverwacht Group. Geological Society of South Africa Special Publication. 2, 113–152.
Wacey, D. (Ed.), 2009. Early Life on Earth: a Practical Guide. Springer, Netherlands, Dordrecht.
Whitney, D.L., Evans, B.W., 2010. Abbreviations for names of rock-forming minerals. American mineralogist 95 (1), 185–187.
Willbold, M., Hegner, E., Stracke, A., Rocholl, A., 2009. Continental geochemical signatures in dacites from Iceland and implications for models of early Archaean crust formation. Earth and Planetary Science Letters 279 (1–2), 44–52.
Wilson, A.H., 2019. The late-Paleoarchean ultra-depleted Commondale komatiites: Earth's hottest lavas and consequences for eruption. Journal of Petrology 60 (8), 1575–1620.
Wilson, A.H., Versfeld, J.A., 1994. The early Archaean Nondweni greenstone belt, southern Kaapvaal craton, South Africa, Part I. Stratigraphy, sedimentology, mineralization and depositional environment. Precambrian Research. 67, 243–276.
Xie, H., Hofmann, A., Hegner, E., Wilson, A., Wan, Y., Liu, D., 2012. Zircon SHRIMP dating confirms a Palaeo- to Mesoarchaean supracrustal terrain in the Kaapvaal craton, southern Africa. Gondwana Research. 21, 818–828.

Further reading

Bédard, J.H., 2018. Stagnant lids and mantle overturns: implications for Archaean tectonics, magmagenesis, crustal growth, mantle evolution, and the start of plate tectonics. Geosci. Front. 9, 19–49.
Drummond, M.S., Defant, M.J., 1990. A model for trondhjemitetonalite- dacite genesis and crustal growth via slab melting: Archean to modern comparisons. J GEOPHYS RES 95, 21503–21521.